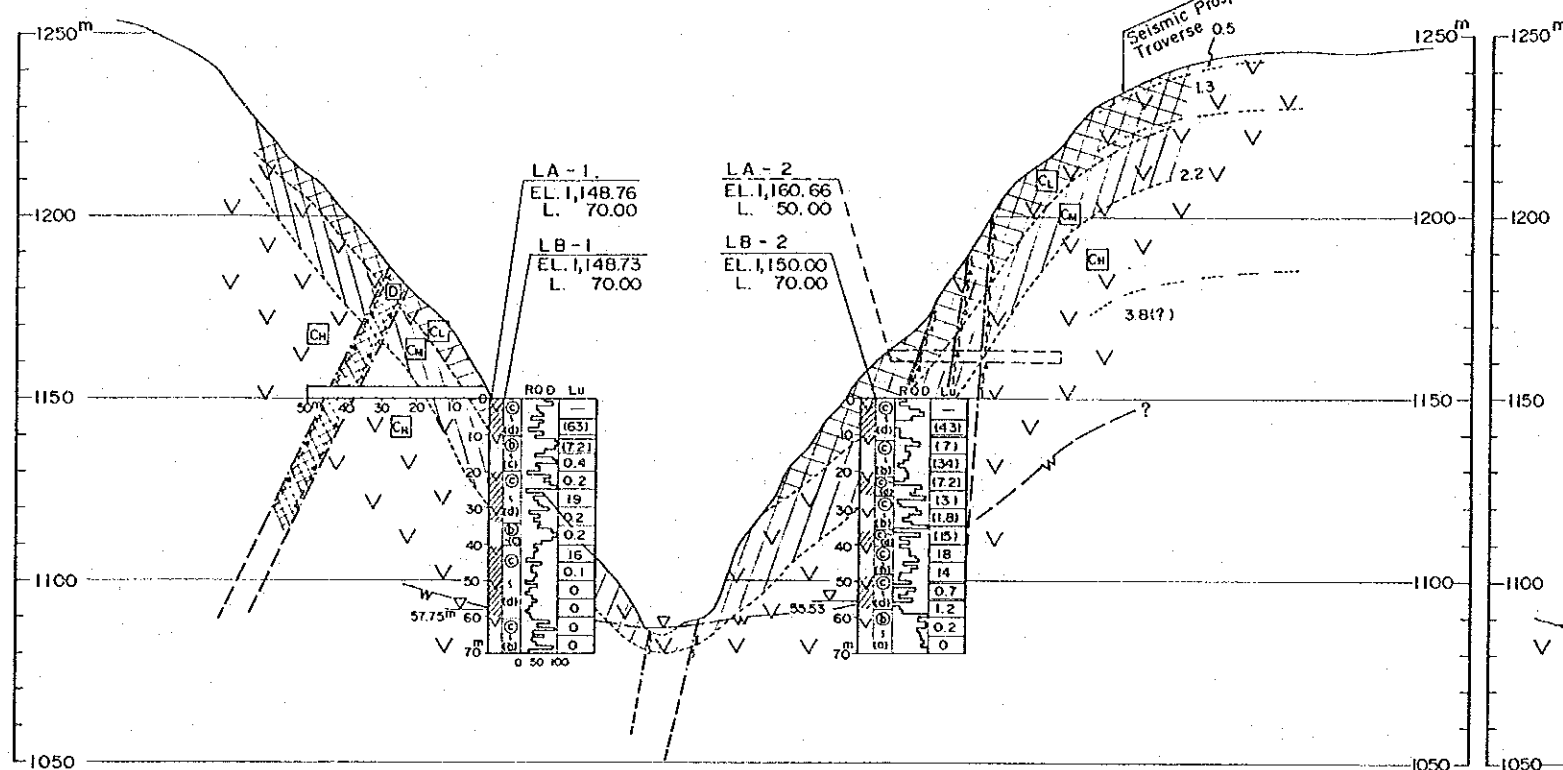
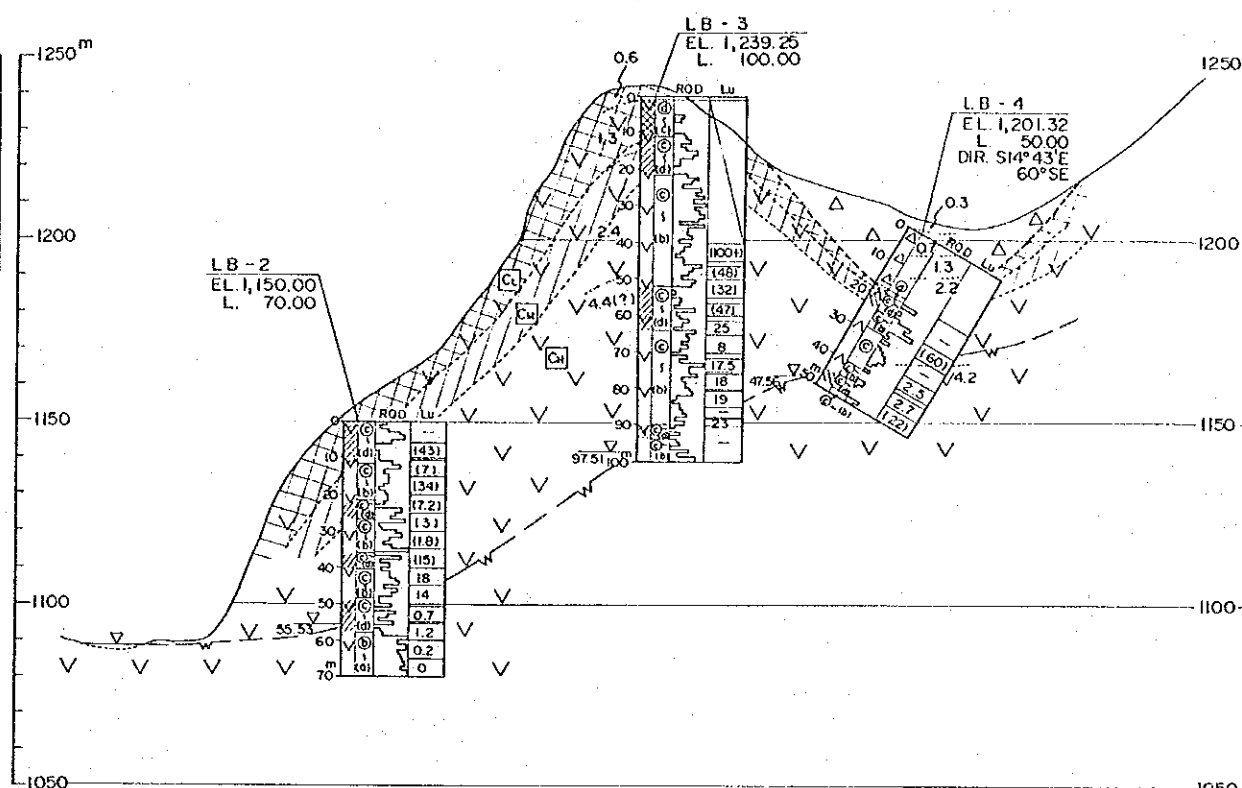


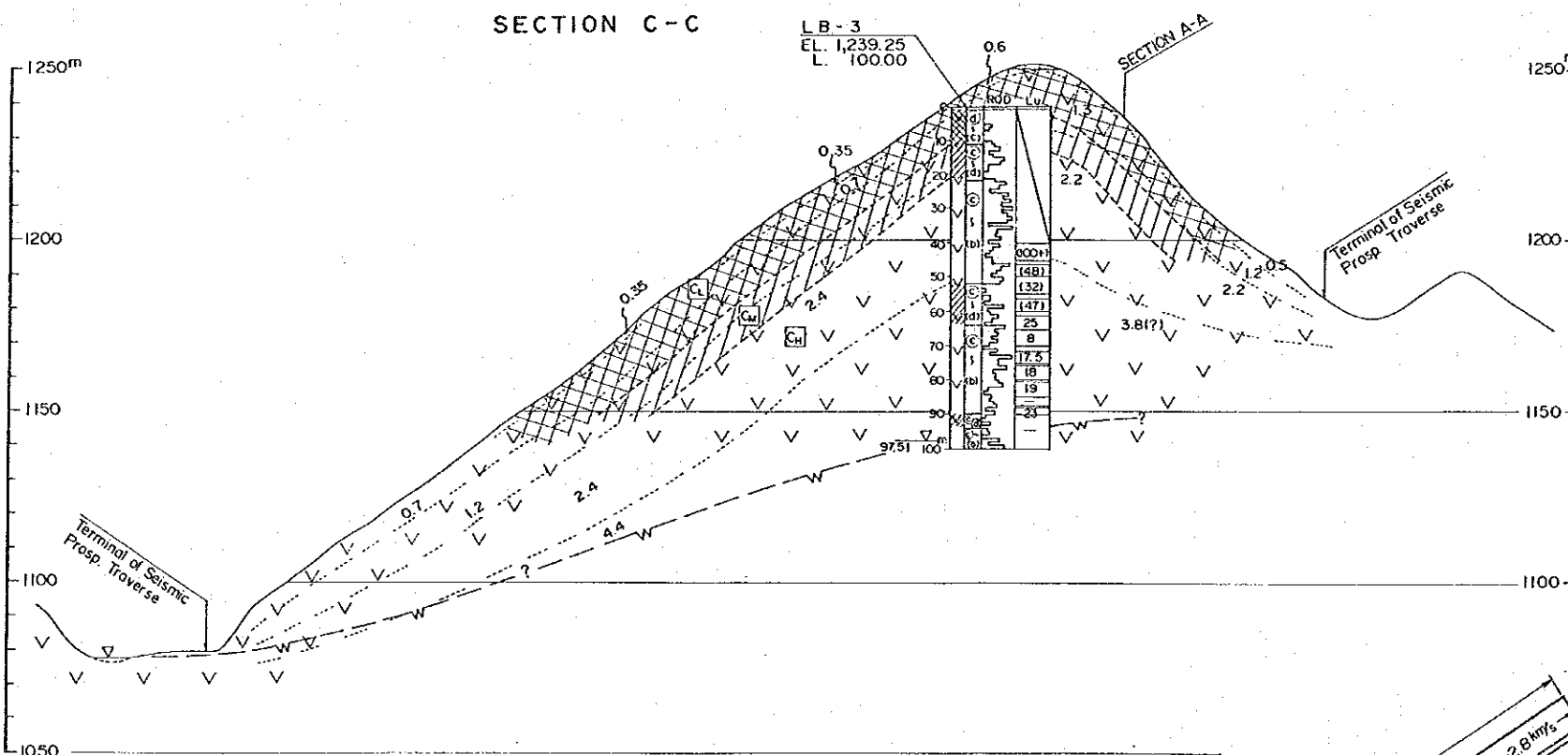
SECTION A - A



SECTION B - B



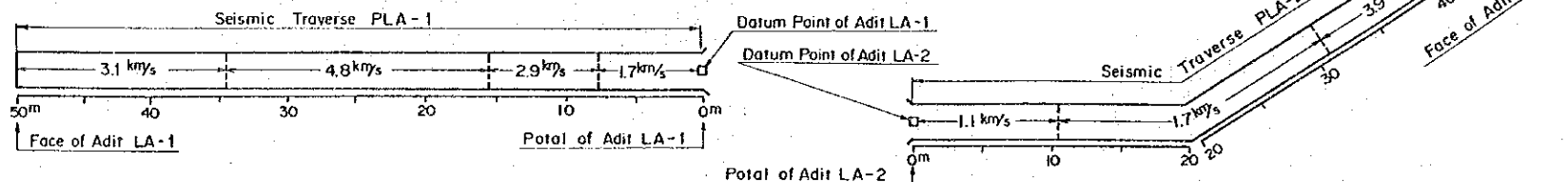
SECTION C - C



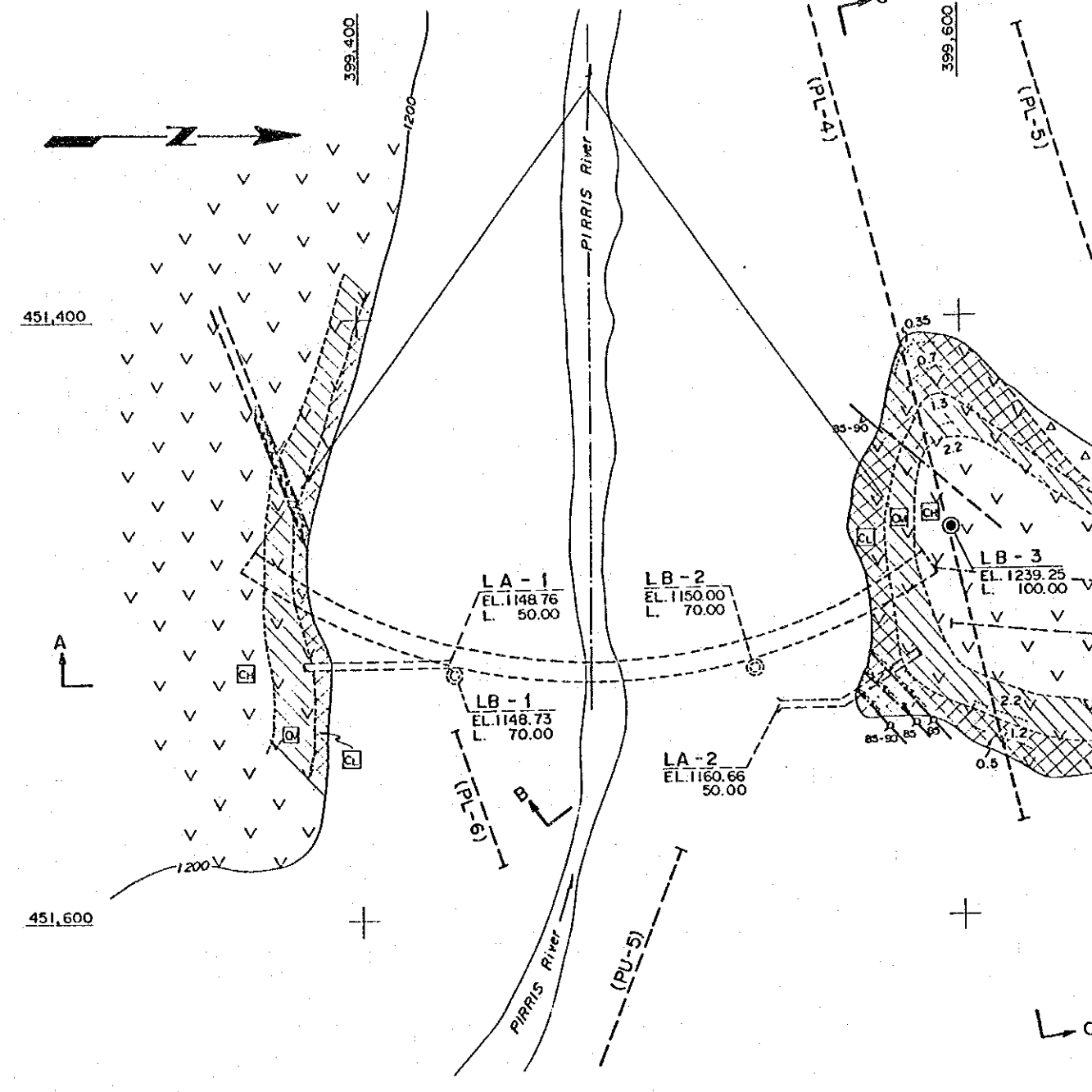
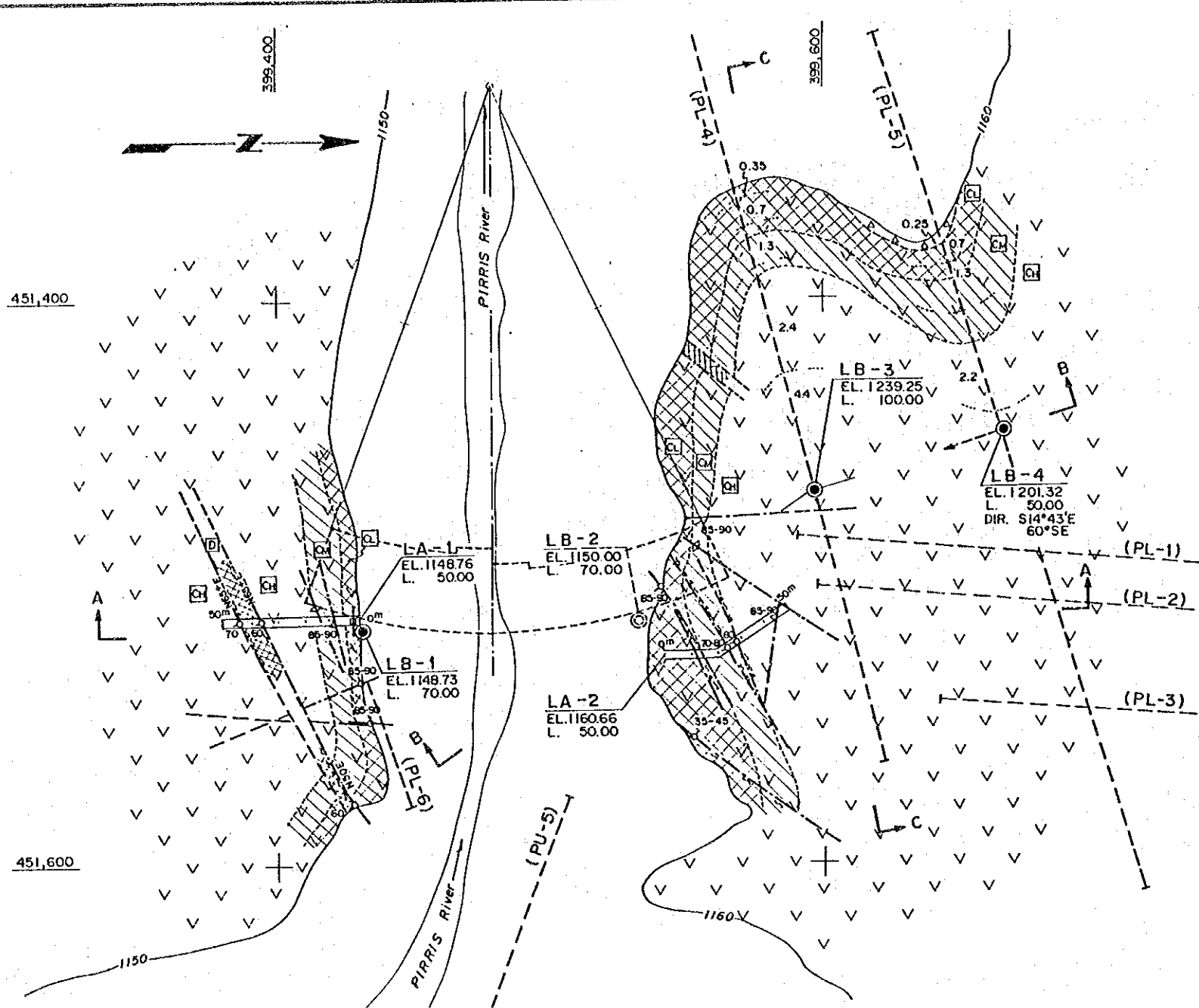
LEGEND

- Talus deposits
- Dolerite ~ Basalt
- Fault
- Geologic boundary
- Boundary of rock mass classification
- Ground water level
- Adit (LA: Adit No., EL: Elevation (m), L: Length (m))
- (Seismic Velocity Distribution) (Velocity (km/s) and boundary of velocity layer)
- (Rock Mass Classification)
 - Somewhat crackly but not loosened rocks
 - Somewhat crackly and slightly loosened rocks
 - Crackly and loosened rocks due to weathering and/or creeping
 - Soft or brittle rocks due to weathering or shearing
- (Drillhole Log)
 - Hole number
 - Elevation of hole head (m)
 - Length drilled (m)
 - Direction and dip of inclined hole
 - Result of Lugeon Test
 - Lu Value assumed from P-Q Curve
 - Lu Value (#min/m/under injection pressure * 10kgf/cm²)
 - Test section
 - Core Evaluation
 - Geologic Log
 - Depth (m)
 - Dolerite
 - Softened or gravelish cores
 - Crackly cores
 - Core Evaluation (See Core Classification and Evaluation)

(Seismic Velocity Distribution in Adit)



REPUBLIC OF COSTA RICA
 PIRRIS HYDROELECTRIC POWER DEVELOPMENT PROJECT
 GEOLOGIC SECTIONS OF DOWN-STREAM DAMSITE
 Fig. 7-6 Date:



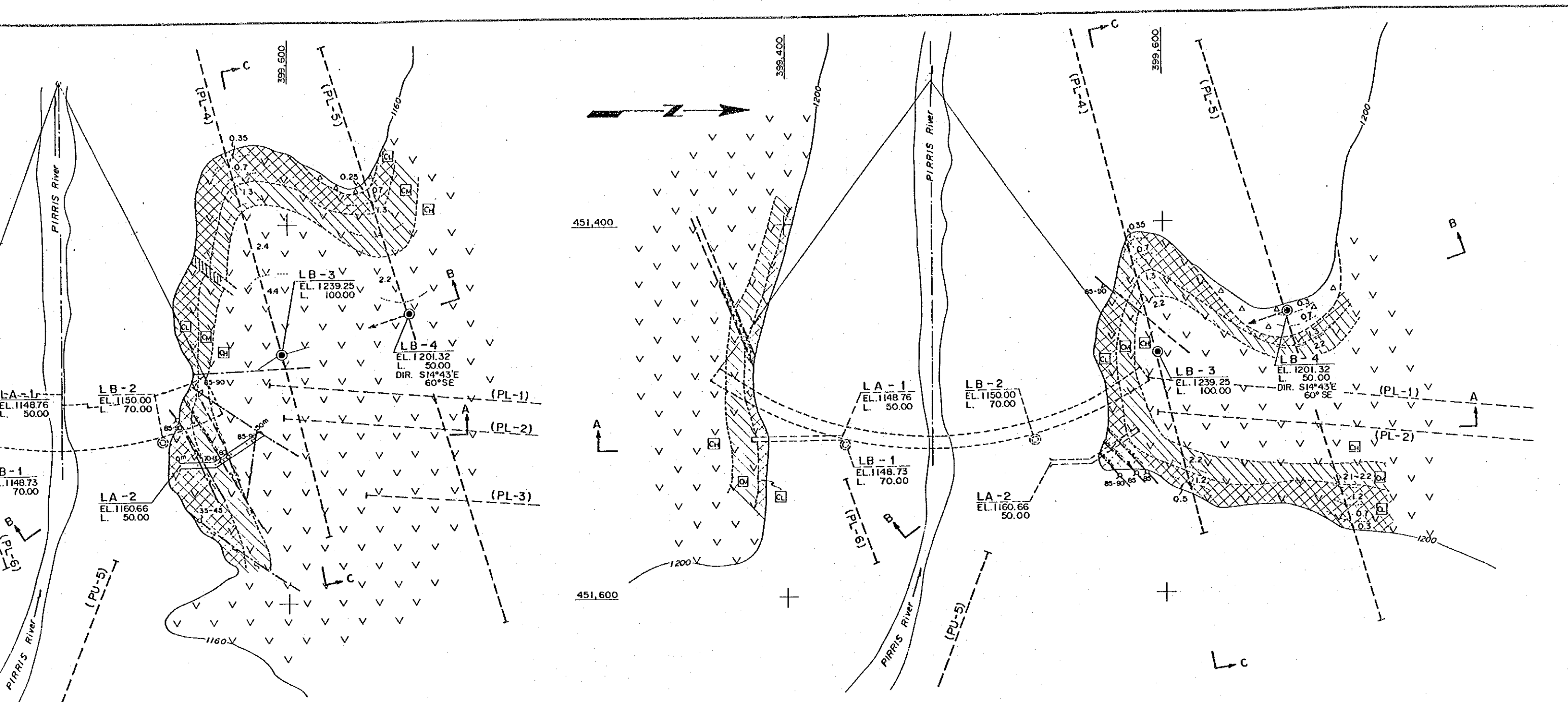
LEGEND

- Talus deposits
- Dolerite ~ Basalt
- Fault and its strike and dip
- Joint and its strike and dip
- Geologic boundary
- Boundary of rock mass classification
- Boundary of seismic velocity (km/s)

- LB-
EL.
L. Drillhole
- LB-
EL.
L. Drillhole (Projected)
- LA-
EL.
L. Adit
- LA-
EL.
L. Adit (Projected)
- (PL-)
Seismic prospecting
traverse (Projected)
- LB - Drillhole No.
- LA - Adit No.
- PL - Traverse No.
- EL. Elevation (m)
- L. Length (m)
- DIR. Direction of inclined hole

(Rock Mass Classification)

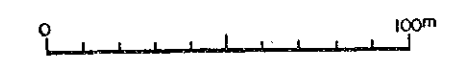
- CH Somewhat crackly but not loosened rocks
- CM Somewhat crackly and slightly loosened rocks
- CL Cracky and loosened rocks due to weathering and/or creeping
- D Soft or brittle rocks due to weathering or shearing



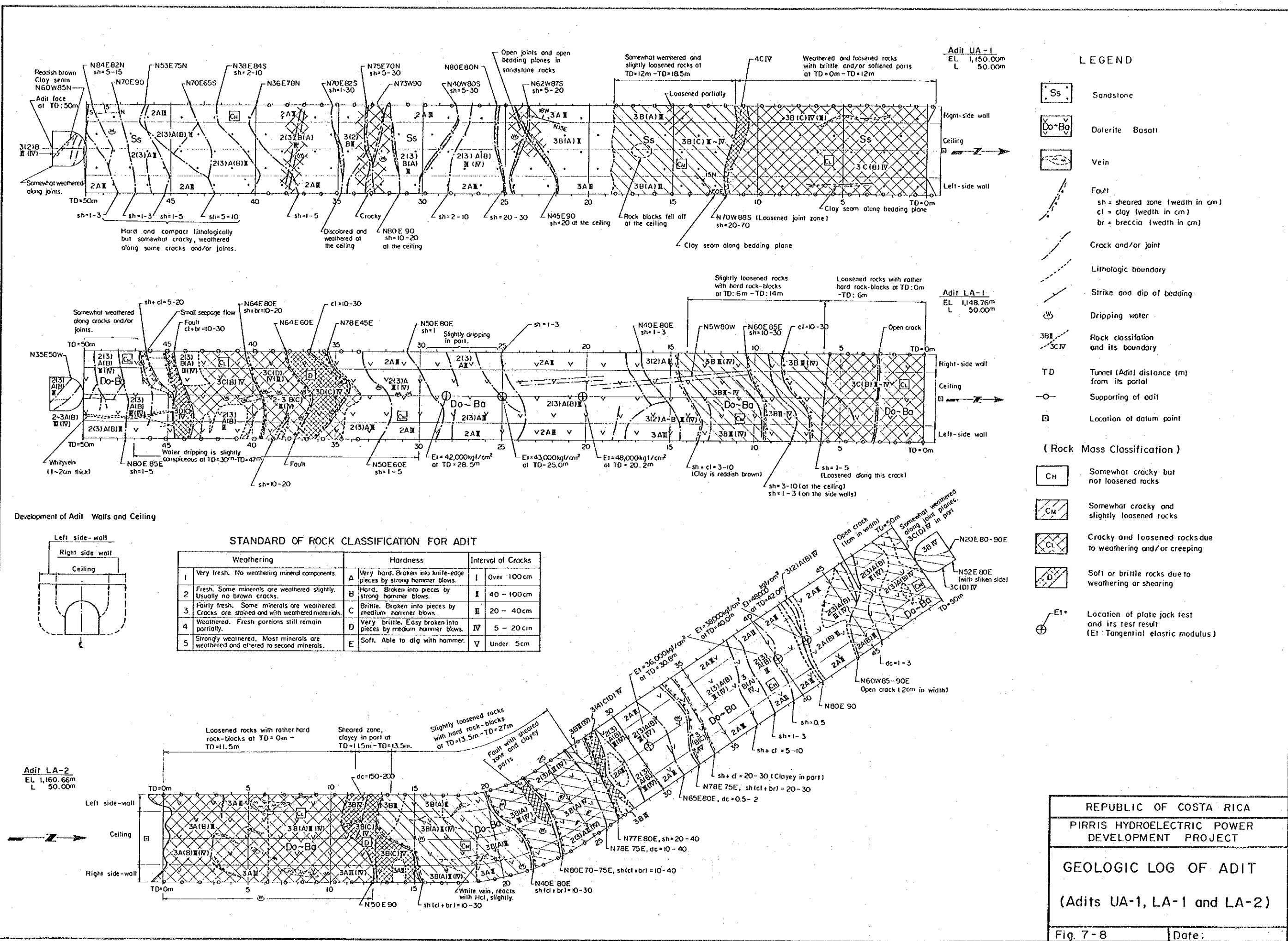
LEGEND

- Alluvial deposits
- Basalt
- Fault and its strike dip
- Fault and its strike dip
- Geologic boundary
- Boundary of rock mass classification
- Boundary of seismic velocity (km/s)
- Drillhole
- Drillhole (Projected)
- Adit
- Adit (Projected)
- Seismic prospecting traverse (Projected)
- LB - Drillhole No.
- LA - Adit No.
- PL - Traverse No.
- EL - Elevation (m)
- L - Length (m)
- DIR. - Direction of inclined hole

- (Rock Mass Classification)**
- CH Somewhat cracky but not loosened rocks
 - CM Somewhat cracky and slightly loosened rocks
 - CL Cracky and loosened rocks due to weathering and/or creeping
 - DL Soft or brittle rocks due to weathering or shearing



REPUBLIC OF COSTA RICA	
PIRRIS HYDROELECTRIC POWER DEVELOPMENT PROJECT	
GEOLOGIC HORIZONTAL SECTIONS OF DOWN-STREAM DAMSITE	
Fig. 7-7	Date;

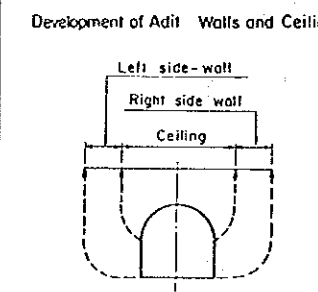


- LEGEND**
- Ss Sandstone
 - Do-Ba Dolerite Basalt
 - V Vein
 - F Fault
 - sh = sheared zone (width in cm)
 - cl = clay (width in cm)
 - br = breccia (width in cm)
 - Crack and/or joint
 - Lithologic boundary
 - Strike and dip of bedding
 - ☉ Dripping water
 - 3BII, 3CIV Rock classification and its boundary
 - TD Tunnel (Adit) distance (m) from its portal
 - Supporting of adit
 - ⊕ Location of datum point

- (Rock Mass Classification)**
- CH Somewhat cracky but not loosened rocks
 - CM Somewhat cracky and slightly loosened rocks
 - CL Cracky and loosened rocks due to weathering and/or creeping
 - D Soft or brittle rocks due to weathering or shearing
 - ⊕ Location of plate jack test and its test result (Et: Tangential elastic modulus)

STANDARD OF ROCK CLASSIFICATION FOR ADIT

Weathering		Hardness		Interval of Cracks	
1	Very fresh. No weathering mineral components.	A	Very hard. Broken into knife-edge pieces by strong hammer blows.	I	Over 100cm
2	Fresh. Some minerals are weathered slightly. Usually no brown cracks.	B	Hard. Broken into pieces by strong hammer blows.	II	40 - 100cm
3	Fairly fresh. Some minerals are weathered. Cracks are stained and with weathered materials.	C	Brittle. Broken into pieces by medium hammer blows.	III	20 - 40cm
4	Weathered. Fresh portions still remain partially.	D	Very brittle. Easy broken into pieces by medium hammer blows.	IV	5 - 20cm
5	Strongly weathered. Most minerals are weathered and altered to second minerals.	E	Soft. Able to dig with hammer.	V	Under 5cm



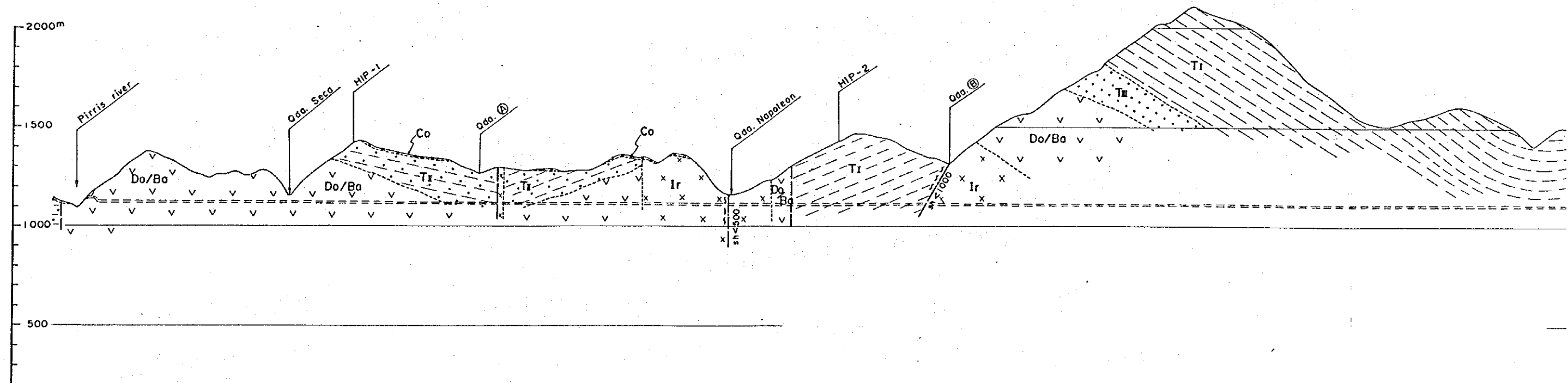
REPUBLIC OF COSTA RICA
PIRRIS HYDROELECTRIC POWER DEVELOPMENT PROJECT

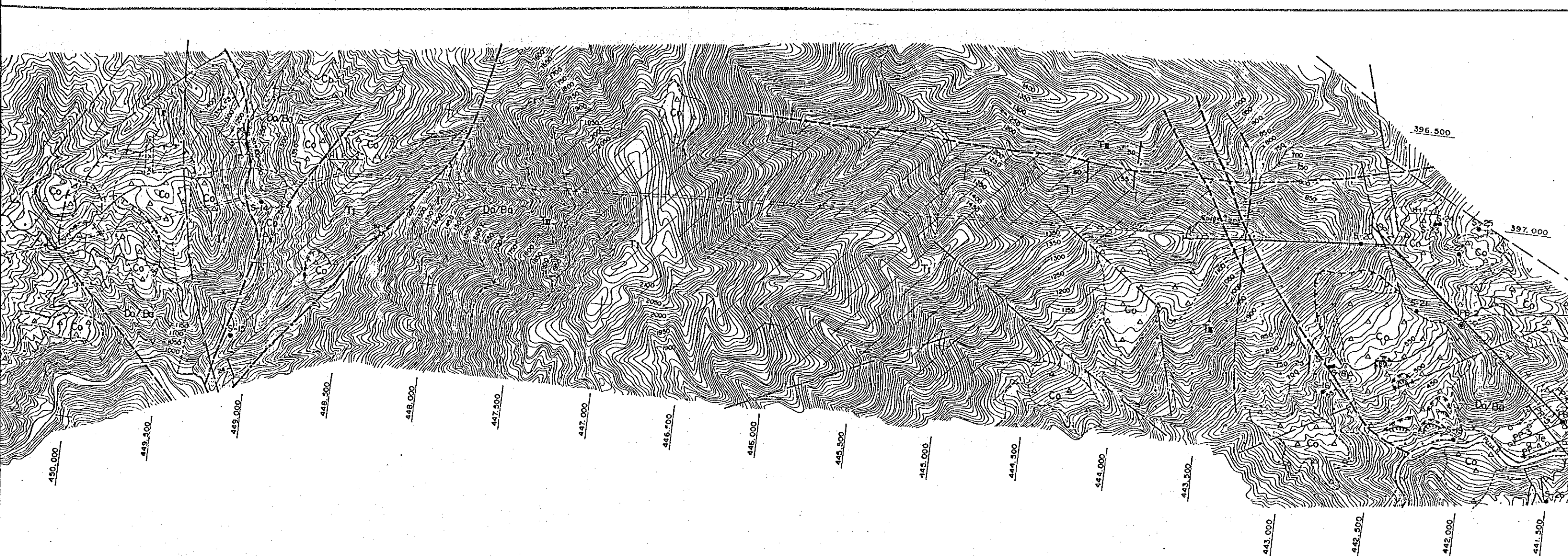
GEOLOGIC LOG OF ADIT
(Adits UA-1, LA-1 and LA-2)

Fig. 7-8 Date: _____

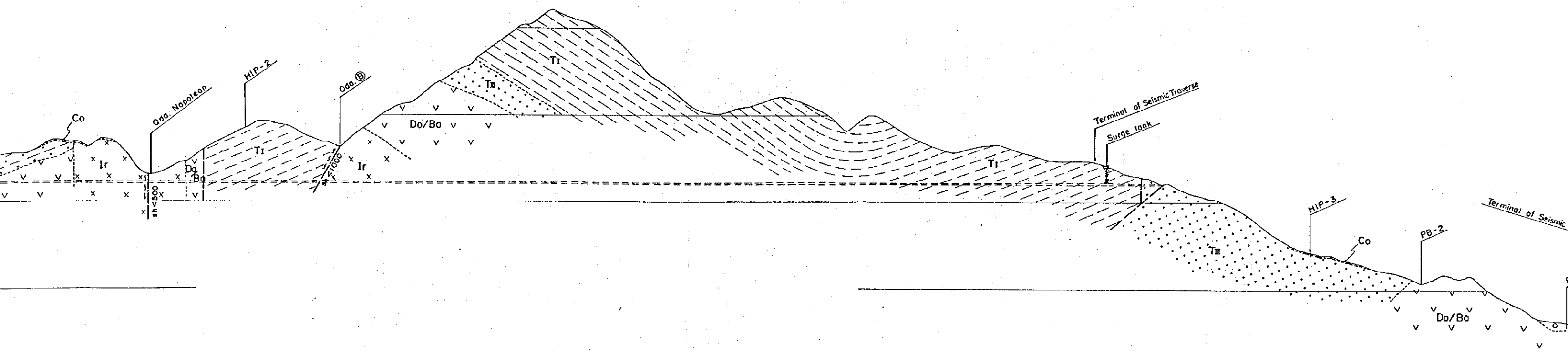


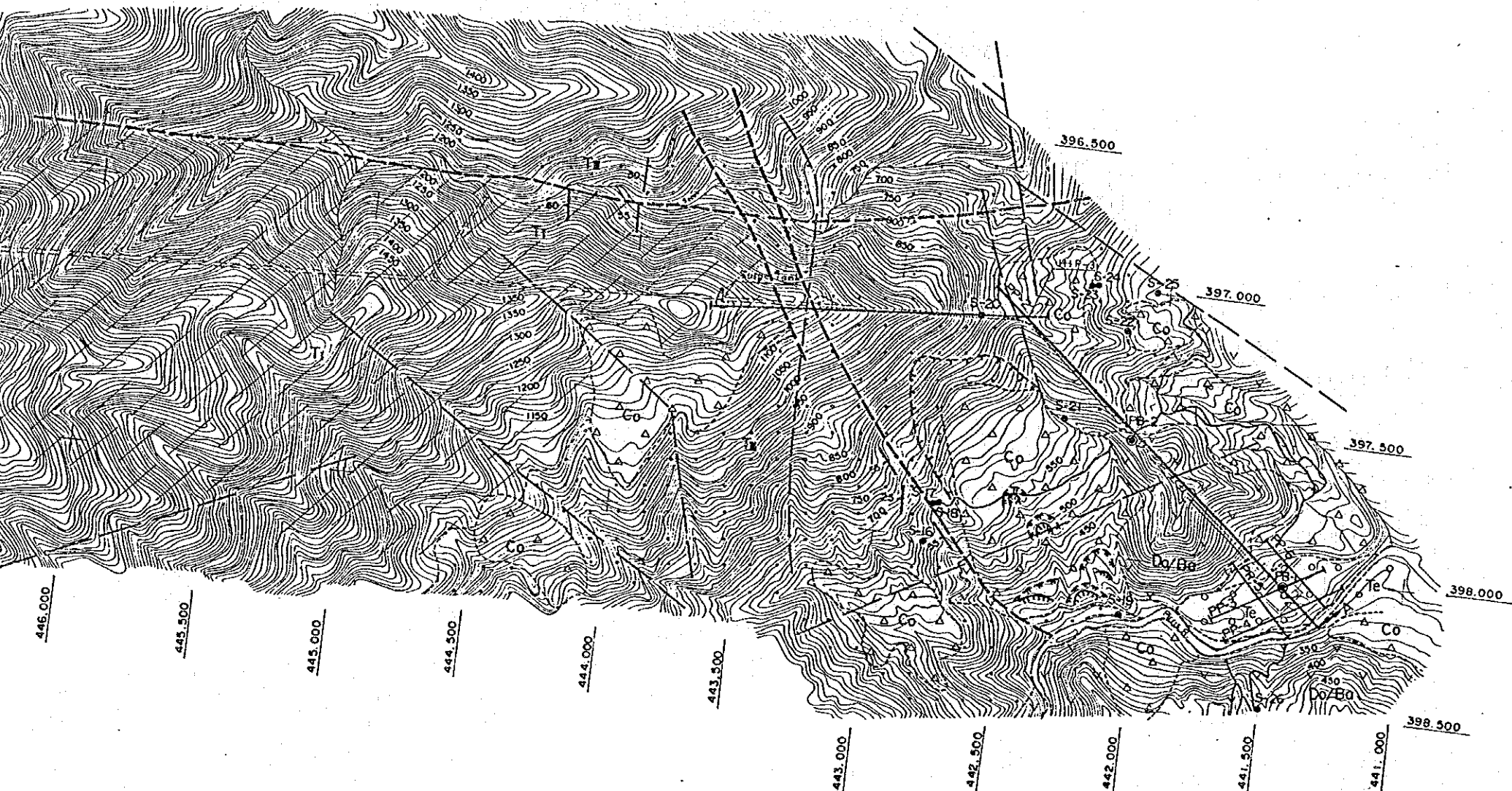
SECTION A-A




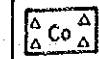
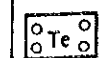


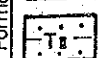

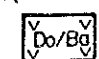
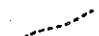

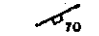
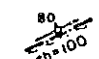



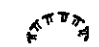
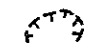

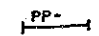
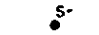


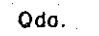


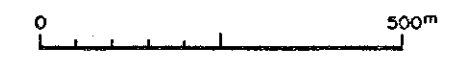
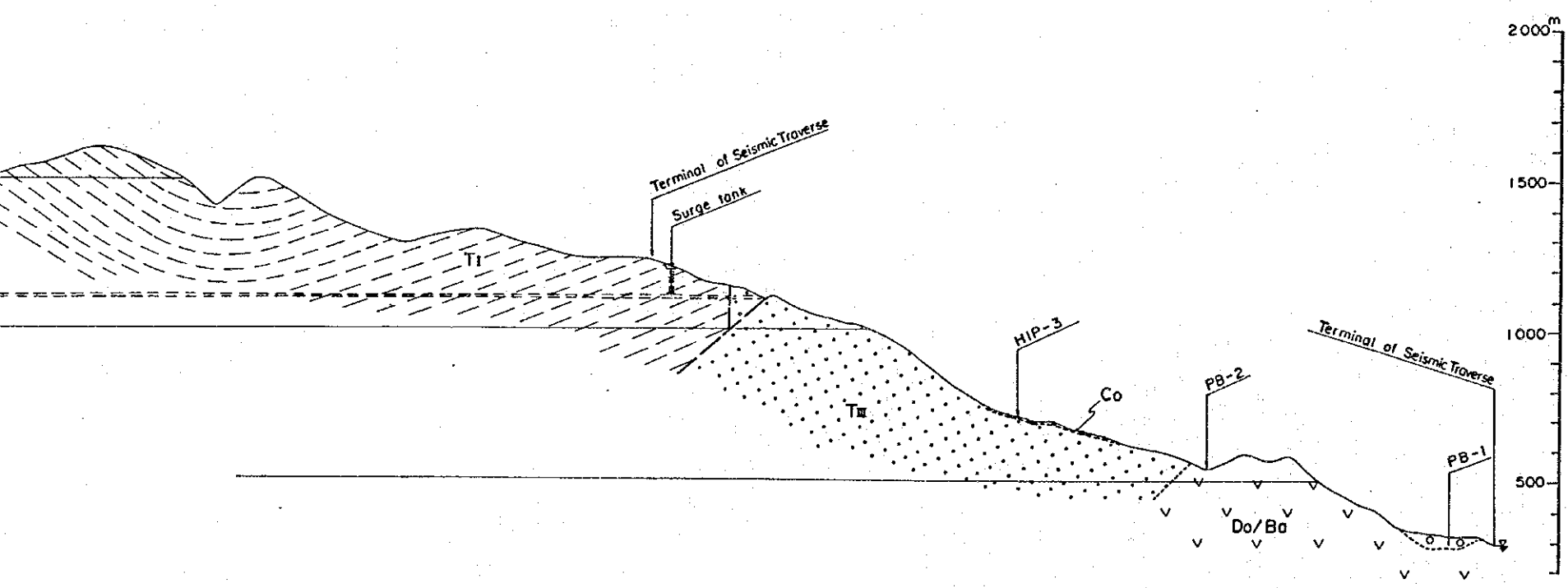
SECTION A-A





LEGEND

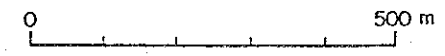
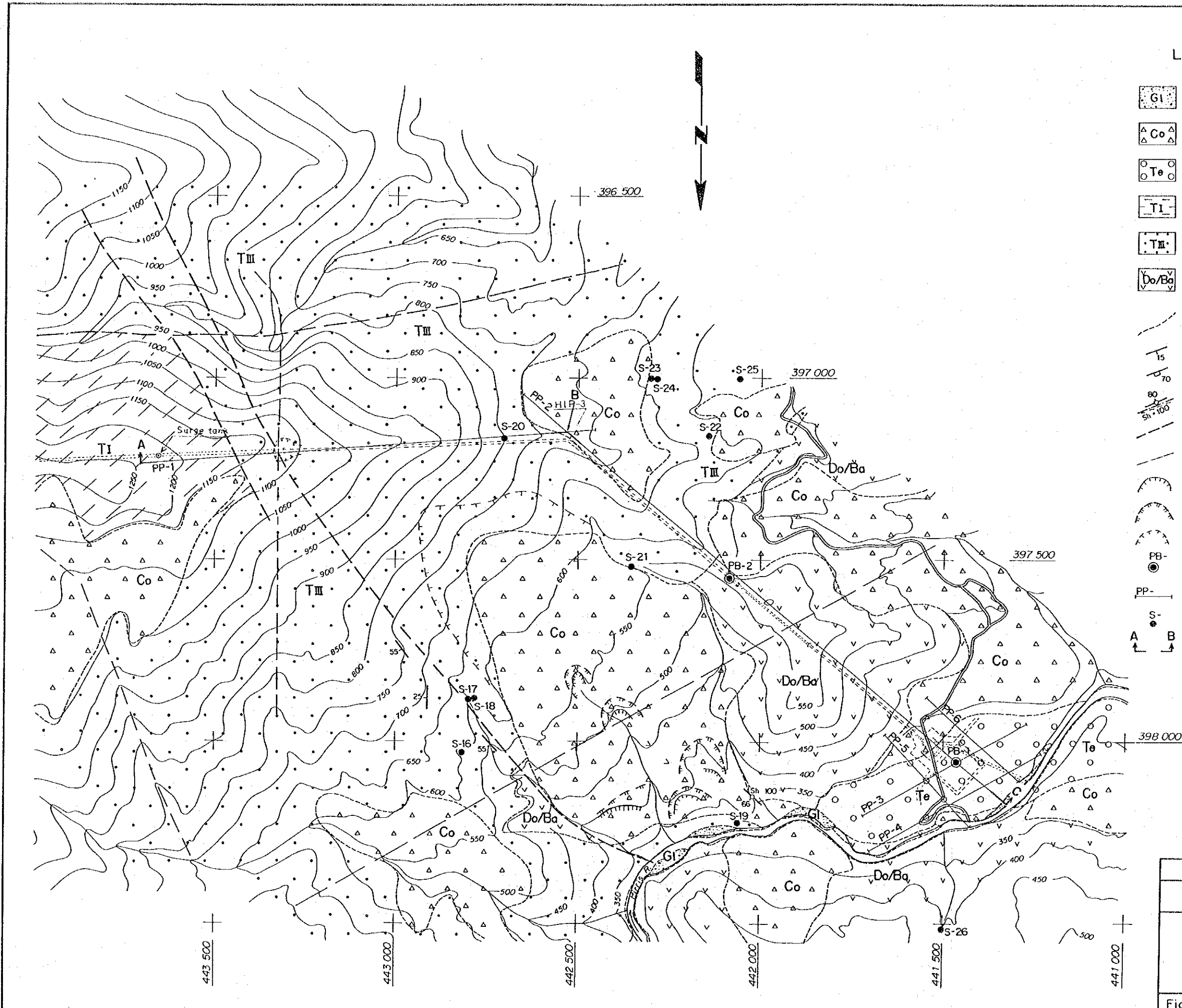
- | | | |
|-------------------|---|--|
| Quaternary |  | Riverbed deposits |
| |  | Colluvial deposits |
| |  | Terrace deposits |
| Tertiary |  | Intrusive rocks |
| |  | Siltstone and claystone |
| |  | Sandstone with shale and conglomerate |
| |  | Sandstone, volcanic sandstone and tuff |
| Eocene - Jurassic |  | Dolerite ~ Basalt |
-
-  Geologic boundary
 -  Strike and dip of bedding
 -  Strike and dip of joint
 -  Strike and dip of fault
sh: width of sheared zone in cm
 -  Assumed fault
 -  Lineament pattern by aero-photo interpretation
 -  Landslide and/or slope failure
 -  Potential landslide and/or slope failure
 -  Probable landslide and/or slope failure by aero-photo interpretation
 -  Drillhole
 -  Seismic prospecting traverse
 -  Sampling locality
 -  Geologic section
 -  Headrace intersection point
 -  Qda. Quebrada (Ravine or small valley)



REPUBLIC OF COSTA RICA	
PIRRIS HYDROELECTRIC POWER DEVELOPMENT PROJECT	
GEOLOGIC PLAN AND PROFILE OF WATER WAY ALIGNMENT	
Fig. 7-9	Date:

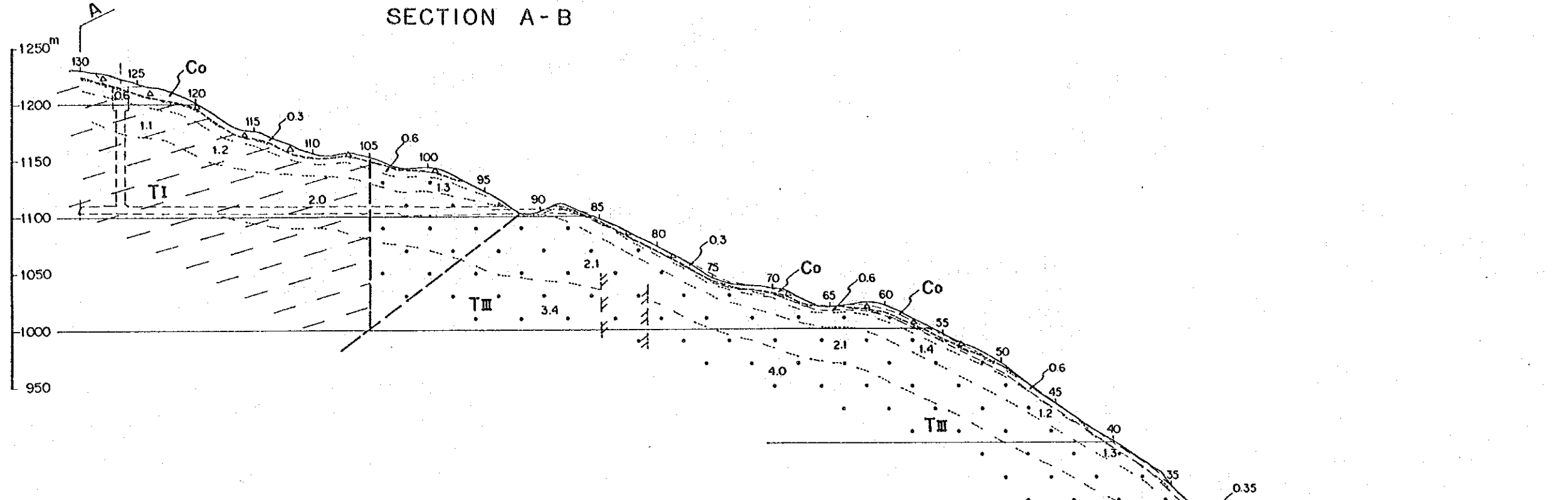
LEGEND

- G Riverbed deposits
- △ Co △ Colluvial deposits
- Te ○ Terrace deposits
- T I Siltstone and claystone
- T II Sandstone, Volcanic sandstone and tuff
- Do/Ba Dolerite ~ Basalt
- Geologic boundary
- Strike and dip of bedding
- Strike and dip of joint
- Strike and dip of fault
Sh: Width of sheared zone in cm
- Assumed fault
- Lineament pattern by aero-photo interpretation
- Landslide and/or slope failure
- Potential landslide and/or slope failure
- Probable landslide and/or slope failure by aero-photo interpretation
- Drillhole
- Seismic prospecting traverse
- Sampling locality
- Geologic section

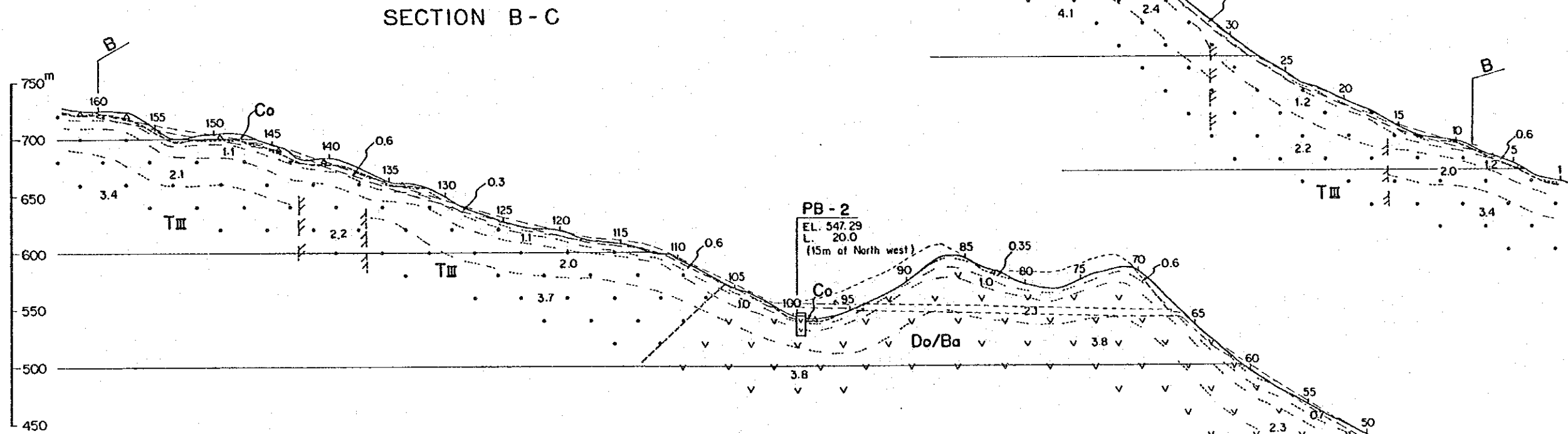


REPUBLIC OF COSTA RICA	
PIRRIS HYDROELECTRIC POWER DEVELOPMENT PROJECT	
GEOLOGIC PLAN OF PENSTOCK ROUTE AND POWERSTATION SITE	
Fig. 7 - 10	DATE:

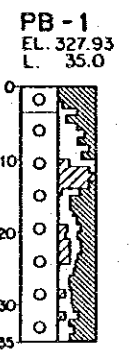
SECTION A-B



SECTION B-C



PB-2
 EL. 547.29
 L. 20.0
 (15m of North west)

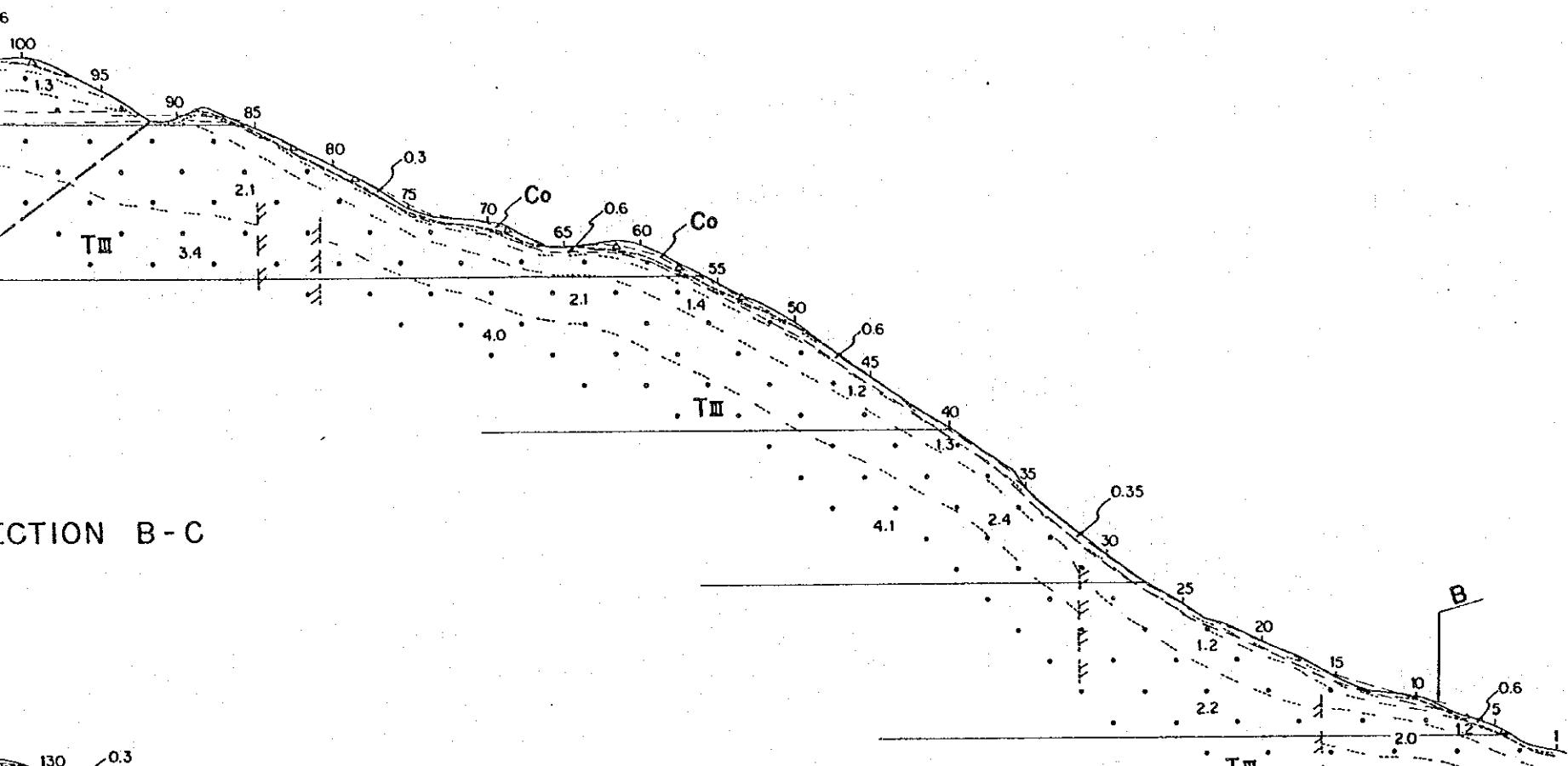


PB-1
 EL. 327.93
 L. 35.0

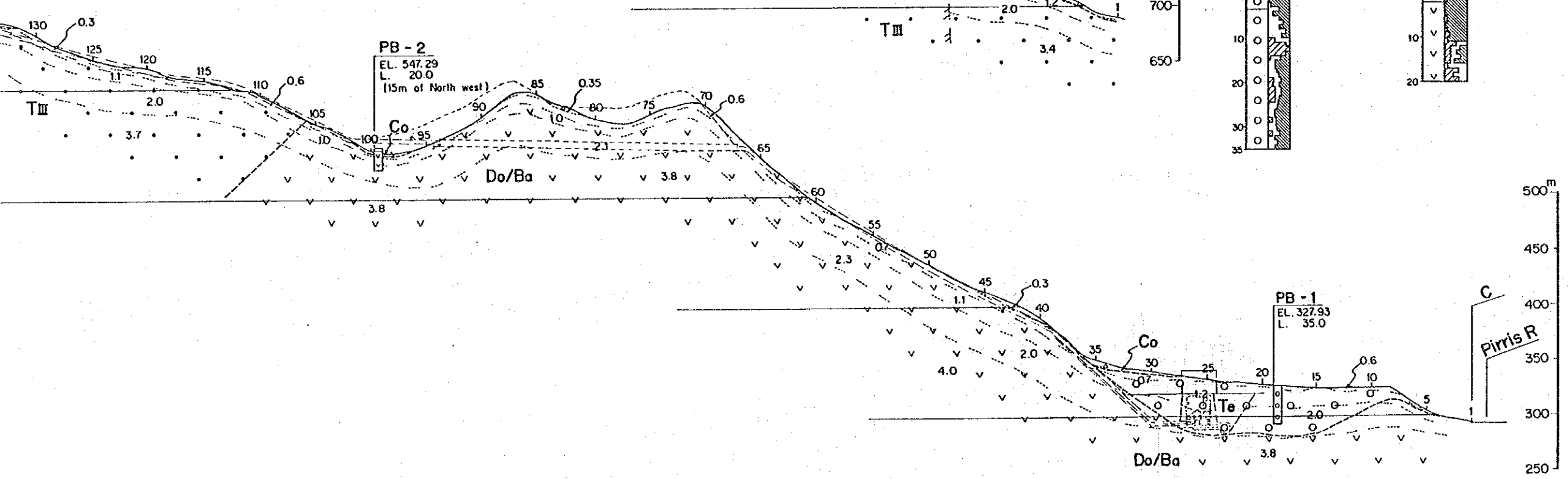
Do/Ba

1
 2
 3
 4
 5
 6
 7
 8
 9
 10
 11
 12
 13
 14
 15
 16
 17
 18
 19
 20
 21
 22
 23
 24
 25
 26
 27
 28
 29
 30
 31
 32
 33
 34
 35
 36
 37
 38
 39
 40
 41
 42
 43
 44
 45
 46
 47
 48
 49
 50
 51
 52
 53
 54
 55
 56
 57
 58
 59
 60
 61
 62
 63
 64
 65
 66
 67
 68
 69
 70
 71
 72
 73
 74
 75
 76
 77
 78
 79
 80
 81
 82
 83
 84
 85
 86
 87
 88
 89
 90
 91
 92
 93
 94
 95
 96
 97
 98
 99
 100

SECTION A-B



SECTION B-C

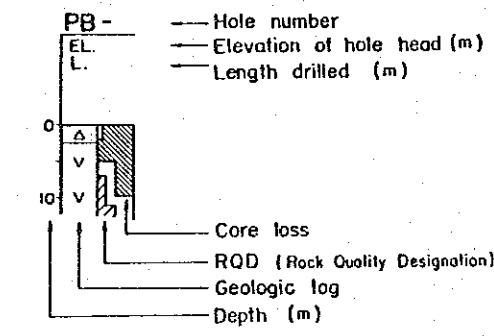


LEGEND

- Colluvial deposits
- Terrace deposits
- Siltstone and claystone
- Sandstone, Volcanic sandstone and tuff
- Dolerite ~ Basalt
- Geologic boundary

(Seismic Velocity Distribution)
 2.0 Velocity (km/s) and boundary of velocity layer
 3.8 Low velocity zone

(Drillhole Log)



Note: SECTION A-B and B-C correspond with seismic Prospecting traverses PP-1 and PP-2 respectively

REPUBLIC OF COSTA RICA
 PIRRIS HYDROELECTRIC POWER DEVELOPMENT PROJECT
 GEOLOGIC PROFILES OF PENSTOCK ROUTE AND POWER STATION SITE

Fig. 7-11 Date ;

7.7 In-situ Rock Foundation Test at Damsite

7.7.1 Introduction

In-situ plate bearing tests were conducted on the rock masses inside exploratory adits at the Pirris Damsite. The purpose of the test is to obtain deformation characteristics of the foundation rocks such as modulus of deformation and modulus of elasticity.

The test was carried out through a contract with a local contractor, Rivas Vargas & Asociados S.A., based on the test method stipulated in the Technical Specifications prepared by the JICA Survey Team, and with the cooperation and guidance of ICE and the JICA survey team.

The test was conducted at a total of six points (see Fig. 7-5), three points each at two locations inside the left- and right-bank exploratory adits (length: 50 m) at the downstream damsite.

The rocks in the exploratory adits on the both banks consisted of dolerite-basalt. The rock masses suitable for the dam foundation can be broadly divided into two classes: C_H class and C_M class of "Rock Mass Classification", as described in 7.5.4. One comprises a sound zone where the rock mass has few fissures or joints, and the rock mass as a whole is tight (C_H class). The other is a zone with slight loosening where fissures or joints are numerous and open cracks are seen even though the rock itself is hard (C_M class).

7.7.2 Plate Bearing Test

(1) Selection of Test Locations

Regarding test locations, the results of geological investigations in the left- and right-bank exploratory adits were first considered, and proposed test sections were selected inside the exploratory adits on deciding to carry out tests on the two representative rock mass classifications of C_H and C_M judged to be suitable as the dam foundation.

The proposed test section of the C_H class was the section from 17.5 m to 33.0 m in the exploratory adit (LA-1) at the left bank. The geology was a rock mass consisting of fresh and hard dolerite-basalt. Fissures exist at intervals averaging 20 to 30 cm and are comparatively few in number. Some have brown color, but are tight. The C_M class was at the section of 30.0 to 45.0 m in the exploratory adit (LA-2) at the right-bank of the damsite. The geology is a rock mass of fresh and hard dolerite-basalt with fissures at average spacing of 10 to 20 cm to be comparatively numerous, with some being brown in color, but they are tight.

The final test locations were selected to be a total of 6 points, three in each rock mass classification upon observing in detail the in-situ rock mass conditions in the Proposed test sections giving consideration to testing operations.

Details of test locations and measuring point names are given in Table 7-15 and Fig. 7-8. Detailed sketches of the test sites are attached to Appendix A-4 (Fig. A-4-6).

(2) Testing Method

The plate bearing test is performed to grasp the deformation characteristics possessed by a rock mass. The test in this case was carried out based on the loading pattern indicated in the Technical Specifications. The contents of the test, as shown in Fig. 7-12, consist of applying initial load, incremental load, sustained load, and maximum load to the rock mass, measuring the loads and displacements of the rock mass to obtain deformation characteristics of the rock mass such as modulus of deformation (D), secant modulus of elasticity (E_s), tangential modulus of elasticity (E_t), and creep factor (C_f).

For the loading apparatus, as shown in Fig. 7-13, a 50-ton hydraulic jack, a bearing plate of diameter 30 cm, and dial gauges (accuracy 1/100 mm) were used.

In general, the maximum load is set at 1 to 2 times the design stress occurred in the rock foundation. Here, the full limit of the jack

capacity was determined to be 65 kg/cm², because 60 kg/cm² is adequate for a dam of 100 m class.

Creep load was 60 kg/cm², and duration period of creep was taken to be 6 hours in consideration of the testing time as a whole. Therefore, the testing time per measuring point became 10 hours as a result.

7.7.3 Test Results and Evaluation

The results and evaluation of the in-situ plate bearing test performed inside the exploratory adits at the right and left banks of the damsite are as described below.

(1) Bearing Capacity of Rock Mass

It was confirmed that both the rock classification C_H and C_M amply have bearing capacities of 65 kg/cm² or more, from the loads and deformation diagrams in result of the plate bearing test as shown in Appendix A-4. The relationship between load and deformation is roughly in a straight line. There are no properties indicating yielding to be seen at all. Although rock masses of the C_H and C_M class in the exploratory adits have fissures or joints, the rock masses are hard and sound.

(2) Plate Bearing Test

The results of plate bearing test indicating the deformation characteristics of the rock masses are shown in Table 7-15, Figs. 7-14, 7-15, and 7-16.

Moduli of deformation (D) of the rock masses were determined in the incremental loads 15, 30, 45, and 60 kg/cm², and secant modulus of elasticity (E_s) and tangential modulus of elasticity (E_t) were obtained in the straight-line section of 20 to 60 kg/cm² in the final loop of the maximum load level (65 kg/cm²).

Further, a value of 0.2 was used for the Poisson's ratio of the rock mass in calculating the various coefficients, since the testing sites were of hard rock (as a measure, unconfined compressive strength of rock more than 500 kg/cm²). Generally in case of hard rock, Poisson's ratio of 0.2 is frequently hypothesized. Assuming a case of increasing the value of Poisson's ratio by 0.05, the variations in the various coefficients will be reductions of roughly 1,000 kg/cm².

On looking at the rock mass characteristics in the test results, the proportion of plastic deformation in total deformation is approximately 37% for C_H class and 56% for C_M class, 1.5 times greater compared with the C_H class. This indicates that C_M class is more subject to the effects of fissures or joints, and the plastic deformation is great.

Moduli of deformation (D) were from 28,000 to 31,000 kg/cm² with C_H class, and 12,000 to 30,000 kg/cm² with C_M class, but as representative values according to overall judgment, they are 30,000 kg/cm² with C_H class, and 14,000 kg/cm² with C_M class.

Tangential moduli of elasticity (E_t) were 42,000 to 48,000 kg/cm² with C_H class, and 36,000 to 48,000 kg/cm² with C_M class, and it is reasonable to consider 43,000 kg/cm² for C_H class and 38,000 kg/cm² for C_M class as representative values. These values also agree well with the modulus of elasticity values for C_H class and C_M class of general rock mass classifications. Further, by general modulus of elasticity is meant this tangential modulus of elasticity (E_t).

As the representative values of secant moduli of elasticity (E_s) they were 38,000 kg/cm² for C_H class and 35,000 kg/cm² for C_M class.

Amounts of creep were 0.04 to 0.06 mm with C_H class, and 0.06 to 0.16 mm with C_M class. The amounts for C_H class were approximately 50% of C_M class. This was slightly on the high side compared with general values, and it is presumed to have been due to the effects of fissures or joints.

Regarding the convergence properties of creep deformation, convergence factors of C_H class were roughly 60% of total creep within 1 hour after

start of creep and 85% at 3 hours, while with C_M class they were 50% and 75%, respectively being convergence factors slower than for C_H class. The amount of creep at 6 hours can be seen to have been the final convergence value for C_H class. For C_M class, it can be considered to have been about 90% of the final convergence value as surmised from the previously-mentioned deformation properties.

Creep factor (C_f) is the proportion of creep to the elastic deformation immediately before creep. The average value of C_f was 15% with C_H class and 31% with C_M class, and not very much different from general values.

These deformation characteristics such as creep quantities, convergence properties, and creep factor (C_f) show well the differences in rock mass classifications.

The following may be said when judged only from the results of plate bearing test.

Regarding classification of the rock masses, all of the characteristics were equal or exceeded the standard values for C_H class and C_M class which are general rock mass classifications and so the classifications are appropriate.

Strength and deformation characteristics of rock masses showed slight effects of fissures or joints, but comprehensively these are hard rock masses. Therefore it is judged that rock mass characteristics are adequate for a dam foundation.

Fig. 7-12 Loading Diagram

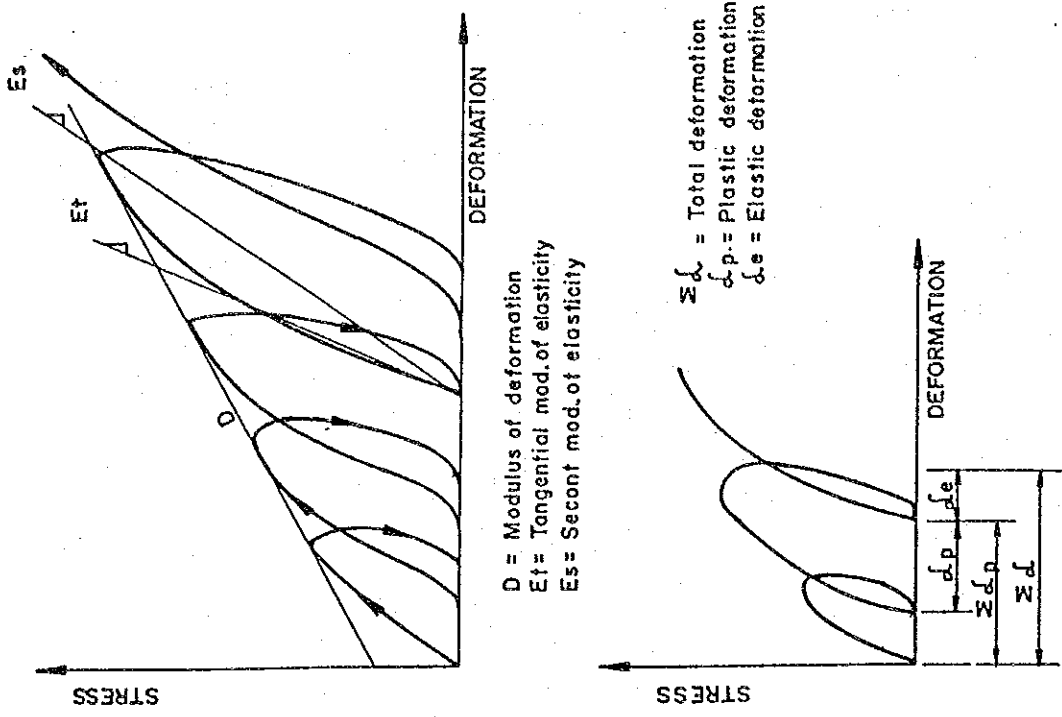
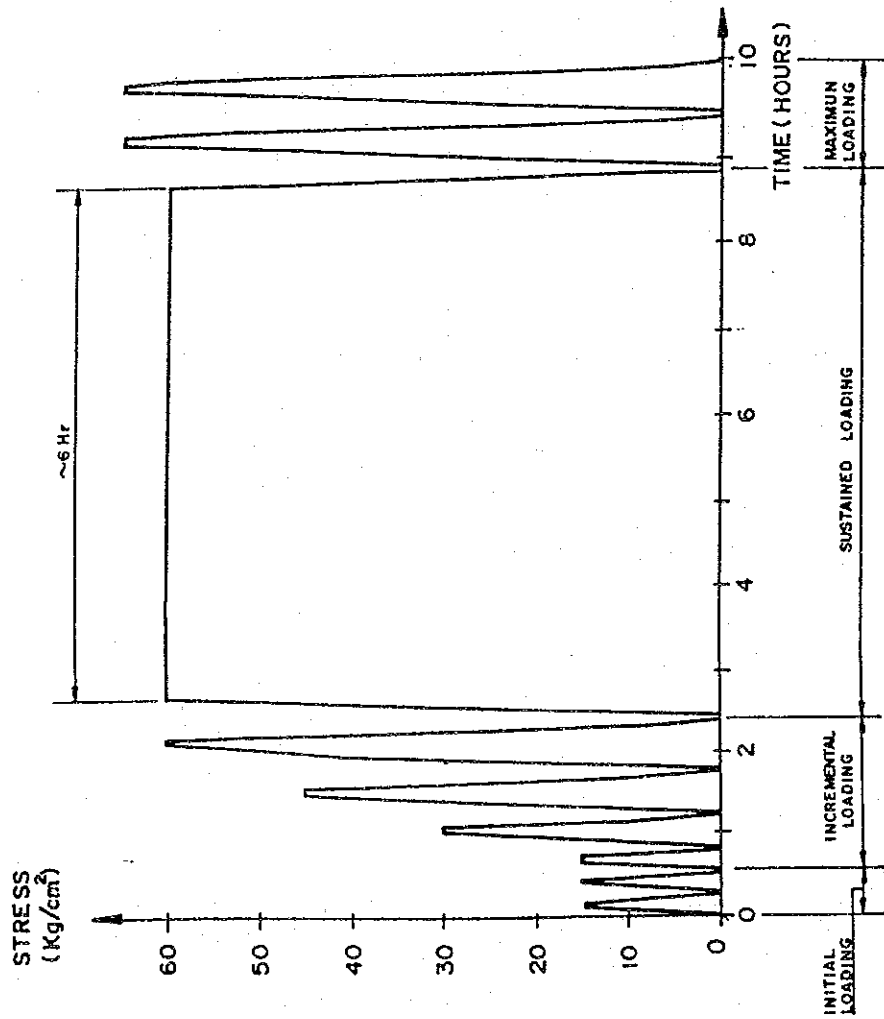


Fig. 7-13 Plate Bearing Test Apparatus

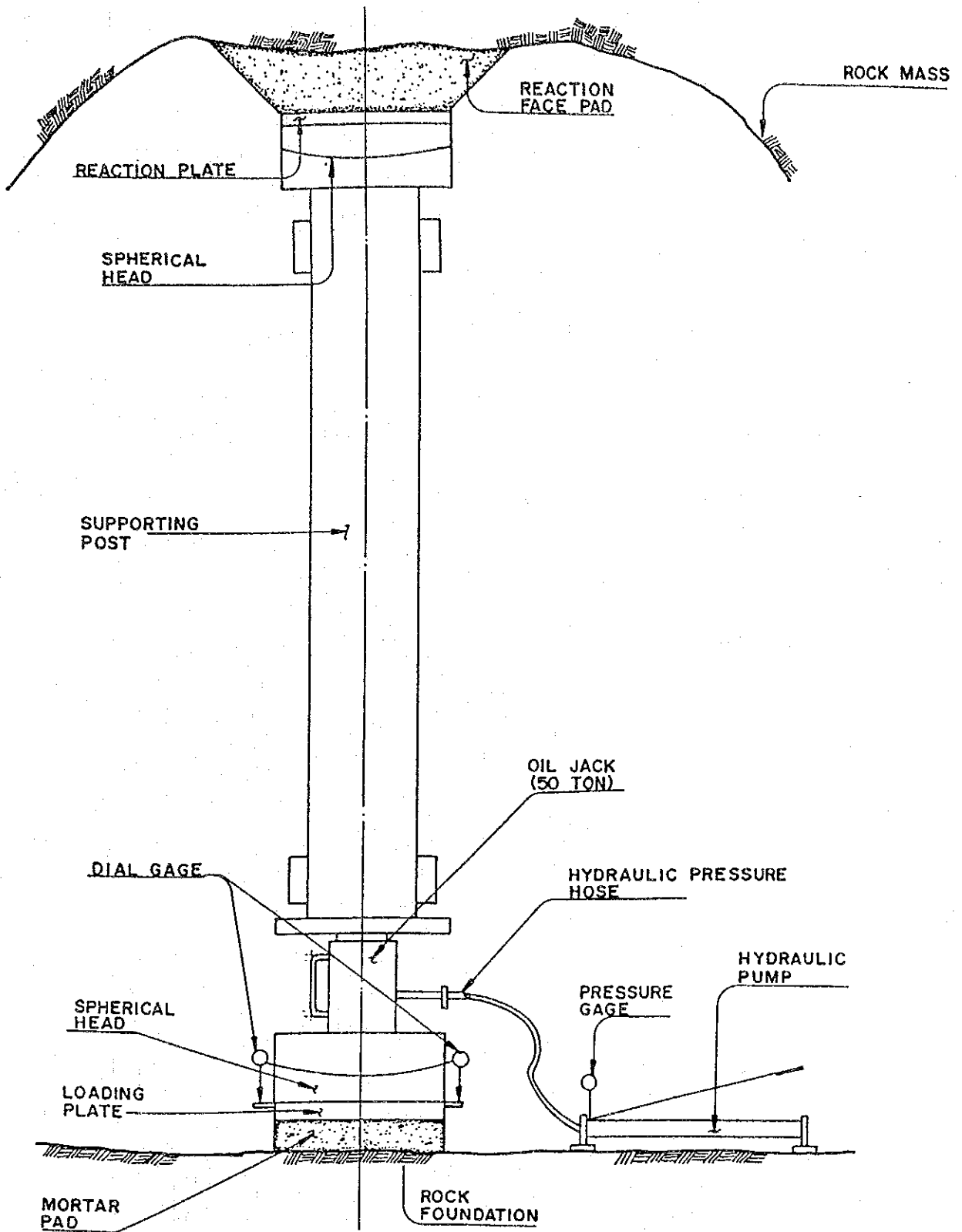


Fig. 7-14 Modulus Characteristics of Rock Foundation

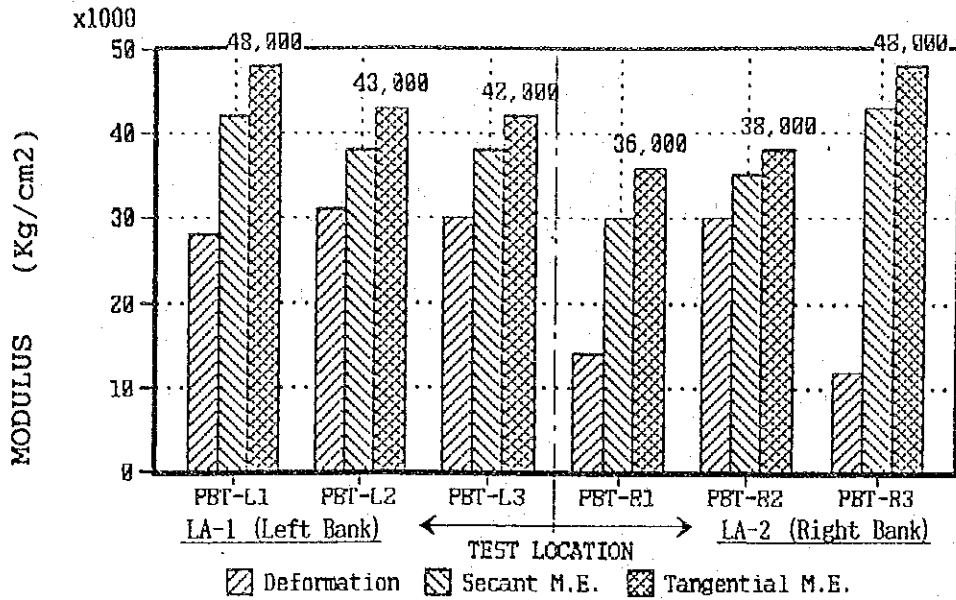


Fig. 7-15 Deformation Characteristics of Rock Foundation

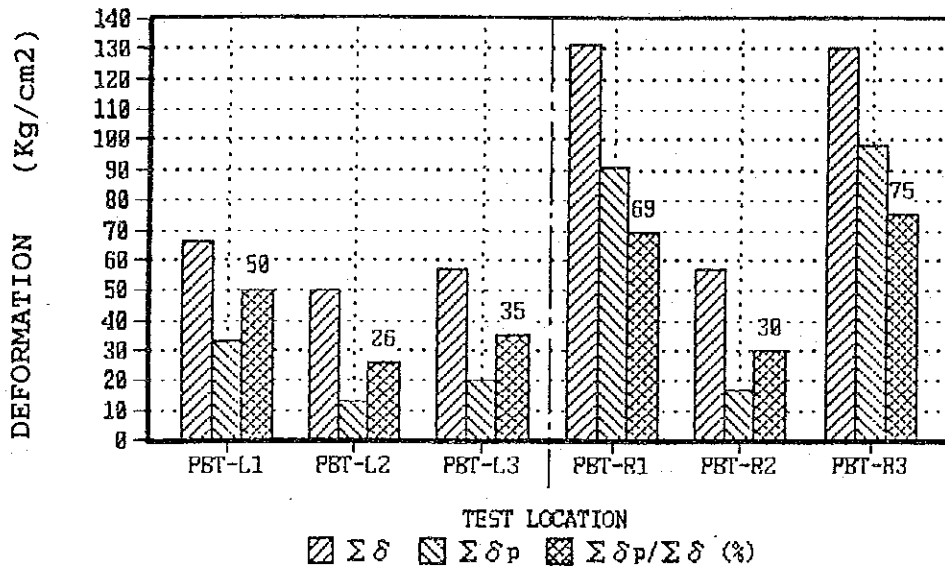


Fig. 7-16 Creep Characteristics of Rock Foundation

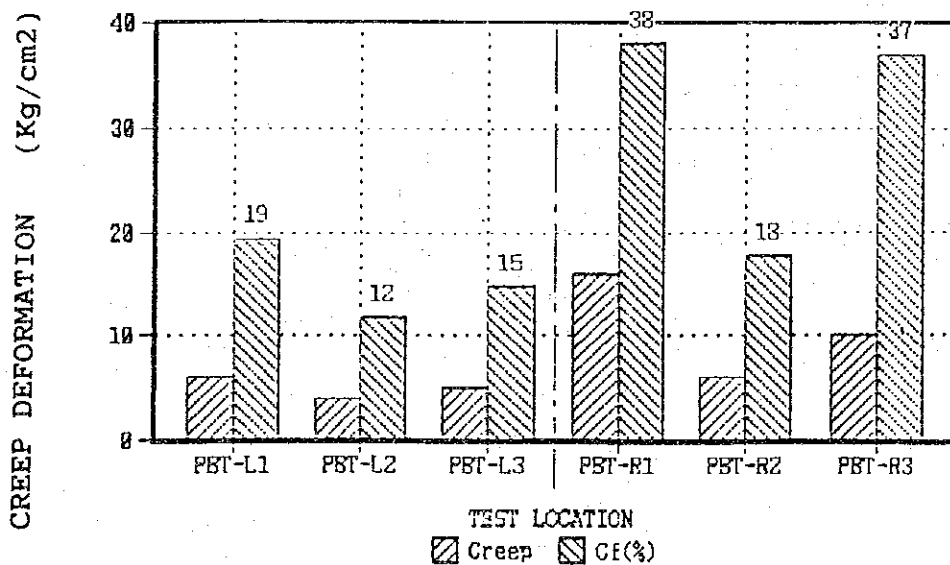


Table 7-15 Result of Plate Bearing Test

Adit	Rock Grade	Measuring Point	Accumulated Distance (m)	Maximum Deformation (1/100mm)	Final Deformation (1/100mm)	$\Sigma \delta p$ ----- (%) $\Sigma \delta$	Modulus of Deformation (kg/cm ²)	Secant Modulus of Elasticity (kg/cm ²)	Tangential Modulus of Elasticity (kg/cm ²)	Creep Deformation (1/100mm)	Creep Factor (%)	Remarks
LA-1	CH	PBT-L1	20.20	66	33	50	28,000	42,000	48,000	6	19	Sound. Little cracks and joint, but tight. Water Nothing.
		PBT-L2	25.00	50	13	26	31,000	38,000	43,000	4	12	
		PBT-L3	28.50	57	20	35	30,000	38,000	42,000	5	15	
		Average		58	22	37	30,000	39,000	44,000	5	15	
LA-2	CM	PBT-R1	30.80	131	91	69	14,000	30,000	36,000	16	38	Sound. Many cracks and joint. Water a little sp-ringing.
		PBT-R2	40.00	57	17	30	30,000	35,000	38,000	6	18	
		PBT-R3	42.00	130	98	75	12,000	43,000	48,000	10	37	
		Average		106	69	58	19,000	36,000	41,000	11	31	

June & July, 1991

7.8 Geophysical Prospecting of Dam and Power Station Sites

7.8.1 Introduction

Surface seismic prospecting with the purpose of exploring the geological conditions of the damsites, and penstock-powerstation site (hereinafter called power station site) from the surface, and in-adit seismic prospecting with the purpose of grasping the properties of the bedrock at the upstream and downstream damsites were carried out, all by ICE.

Measurement work was done by ICE, with analyses performed by ICE with the cooperation of the JICA Team, and evaluations of the prospecting results were made by the JICA Team.

7.8.2 Selection of Prospecting Locations

(1) Selection of Prospecting Location

Surface seismic prospecting was performed at the damsites and the power station site.

The arrangements of seismic prospecting traverses at the damsites are as shown in Appendix A-5-1. There was a total of 12 prospecting traverses provided, six at the upstream damsite and six at the downstream damsite. Of these, PU-4 and PU-5, and PL-1 to PL-5 were concurrently for investigation of construction materials borrow areas.

The layout of prospecting traverses at the power station site is as shown in Appendix A-5-2. Two prospecting traverses were arranged along the penstock route and four on the river terrace of the power station site, a total of six.

In-adit seismic prospecting was done inside Adit UA-1, on the left bank of the upstream damsite and Adits LA-1 and LA-2, on the left bank and right bank of the downstream damsite, respectively. Locations of these adits are as shown in Fig. 7-3 and 7-5.

(2) Investigation Quantities

The investigation quantities, the coordinates and elevations of beginning points and ending points of the individual prospecting traverses are compiled together in Appendix A-5-3.

7.8.3 Prospecting Method

(1) Measurement Method

Surface seismic prospecting was done according to the method described below using the measuring instruments shown in Table 7-16.

Table 7-16 List of Seismic Prospecting Instrument

Name	Specification	Remarks
Amplifier	No. of channels : 24 Frequency Response : 2 - 300 Hz Gain : 120 dB	SIE (RA-44A)
Recorder	No. of channels : 26 Paper drive speed : 6 - 24 ips Timing line : 5 or 10 ms	SIE (R-6B)
Geophone	Frequency : 14 Hz Coil resistance : 350 - 400 Ω	Geo - Source
Blaster	Capacitor discharge type (170 VDC) Test circuit Timebreak circuit	SIE (PCD-49)
Takeout cable	12 takeouts x 2 Spacing : 20 m	
Signal Processing and Enhancement Seismographs*	No. of channels : 12 Record Length : 48 to 4,800 ms Record Resolution : 959 samples per channel Enhancer resolution 16 bits Input memory resolution 8 bits Gain : 24 to 108 db in 6 db step Display : Cathode Ray Tube (228 mm) Hard Copy : Thermal Printer (110 mm wide) Power Requirements : 12 volts, DC	BISON (8012A)
Geophone*	Frequency : 14 Hz	Mark Products
Triger*	Solid state triger	BISON
Takeout cable*	12 takeouts	NINBUS

Note: * These instruments were used for in-adit prospecting.

Receiving points were set up on prospecting traverse by stadia surveying at every approximate 5 m (horizontal distance) at the damsites, and every approximate 10 m at the powerstation site. The number of shot points per spread was made a minimum of four locations. The spacings between shot points were approximately 60 m at the damsites and 70 to 110 m at the powerstation site. Explosive was used for seismic energy source, with this exploded underground or underwater to generate elastic waves. The lengths of single spreads were approximately 110 m at the damsites and approximately 220 m at the powerhouse site.

In-adit seismic prospecting was carried out by the method below using the measuring instruments listed in Table 7-16.

Seismic prospecting traverses were laid out at inverts along adit walls showing little loosening. Receiving points were set at every 2.5 m (horizontal distance) on the prospecting traverses. Shot points were arranged at the two ends of prospecting traverses and in between. For seismic energy source, the method of striking strongly by hammer was used. Since the exiting energy was manual and small, input signals were added and multiplied using a signal enhancement, that is, a stacking method was applied.

(2) Analysis Method

Seismic prospecting is a method to presume geological conditions of underground materials by analyzing change in velocity of seismic wave (or primary elastic wave). The change comes from the difference in physical property. The accuracy depends on measurement technique and such factors as geological characteristics (velocity changes gradually to the vertical direction) and complicated topographical/geological structure. Analytical theory has not yet dealt with these factors. Therefore, the analyzed velocity and the form of velocity layer are generally averaged.

For the analyses of records from the Pirris prospecting works, Hagiwara's Method and its expanded version were used. These methods are

generally applied to a refraction prospecting aiming at grasping the conditions of the basement of civil structures.

7.8.4 Result and Evaluation of Prospecting

(1) Surface Seismic Prospecting

The individual seismic profiles are shown in Appendix A-5-4 (Sheet No. 1 to Sheet No. 16), and time-distance plots in the Appendix A-5-5 (Sheet No. 1 to Sheet No. 14). The accuracies of analyses in the seismic profiles were expressed by the method below.

- Layer boundaries are shown by solid lines when it is possible to obtain the depth travel time, and moreover, the analysis results are of high degree of accuracy.
- When the depth-travel time of the basement cannot be obtained, the velocity travel time of an adjacent location where depth travel time has been obtained is extended to estimate the depth travel time and obtain the depth. In this case, the boundary of the basement is shown by a broken line.
- When the relief of the topography is severe or the geological structure is complex, or when measurement errors are large so that analyses are difficult to make, analyses are performed referring to intersecting seismic profiles and other geological investigation data, and the results are shown by a dot-dash line.

The subsurface structure at the investigation sites was classified as consisting of four to five velocity layers. The velocity layer classifications at the individual prospecting lines are given in Table 7-17, and the velocity layers of the individual prospecting lines are described below.

Table 7-17 Classification of Velocity Layer

Line	Layer	1st Layer	2nd Layer	3rd Layer	4th Layer	Basement	Low Velocity Zone
PU-1 (PS-12)	Velocity Thickness	0.35~0.4km/s 5.0m	0.8~0.85km/s 10m	1.3~1.4km/s 21m	2.3~2.4km/s 36m	4.4km/s	--
PU-2 (PS-11)	Velocity Thickness	0.25~0.35km/s 5.0m	0.6~0.7km/s 13m	1.2~1.3km/s 25m	2.2~2.4km/s 25m	4.6km/s	--
PU-3 (PS-10)	Velocity Thickness	0.35~0.4km/s 7.0m	0.6~0.7km/s 9.0m	1.2km/s 23m	2.2~2.3km/s 26m	4.6km/s	--
PU-4 (PS-9)	Velocity Thickness	0.2~0.3km/s 3.0m	0.5~0.6km/s 6.0m	1.0~1.2km/s 17m	2.0~2.1km/s 32m	4.6km/s	--
PU-5 (PS-8)	Velocity Thickness	0.2km/s 2.0m	0.45~0.6km/s 8.5m	0.9~1.0km/s 20m	2.0~2.4km/s 27m	4.6, 4.9km/s	2.4km/s
PU-6 (PS-13)	Velocity Thickness	0.15~0.3km/s 1.5m	0.6km/s 5.5m	1.2km/s 8.0m	2.2km/s 11~16m	4.4km/s	2.5km/s
PL-1 (PS-1)	Velocity Thickness	0.15~0.25km/s 3.0m	0.5~0.6km/s 11m	1.2~1.3km/s 15m	2.1km/s 22~42m	3.6km/s	--
PL-2 (PS-2)	Velocity Thickness	0.15km/s 2.0m	0.5km/s 3.0m	1.0~1.3km/s 17m	2.0~2.2km/s 17~36m	3.8km/s	--
PL-3 (PS-3)	Velocity Thickness	0.2km/s 1.5m	0.4~0.6km/s 4.0m	1.1~1.2km/s 10m	2.0~2.1km/s 12~27m	3.8km/s	--
PL-4 (PS-4)	Velocity Thickness	0.3~0.35km/s 3.0m	0.5~0.7km/s 7.0m	1.2~1.3km/s 17m	2.2~2.4km/s 38m	(3.8), 4.4km/s	--
PL-5 (PS-6)	Velocity Thickness	0.25~0.3km/s 4.0m	0.6~0.7km/s 5.0m	1.2~1.3km/s 13m	2.0~2.2km/s 32m	(3.8), 4.2km/s	2.7km/s
PL-6 (PS-7)	Velocity Thickness	0.4km/s 1.5m	--	1.1km/s 5.0m	1.7km/s	--	--
PP-1 (P-7)	Velocity Thickness	0.3~0.35km/s 11m	0.6~0.7km/s 9.0m	1.1~1.4km/s 28m	2.0~2.4km/s 17~58m	3.4~4.1km/s	2.2, 2.6km/s
PP-2 (P-5)	Velocity Thickness	0.3~0.35km/s 5.0m	0.6~0.7km/s 8.0m	1.0~1.2km/s 25m	2.0~2.3km/s 10~30m	3.4~4.0km/s	--
PP-3 (P-3)	Velocity Thickness	--	0.5~0.65km/s 4.0m	1.1~1.4km/s 19m	2.0~2.1km/s 22~45m	4.1km/s	--
PP-4 (P-4)	Velocity Thickness	--	0.4~0.5 km/s 4.0m	1.1~1.2km/s 12m	2.0~2.3km/s 5.0~27m	4.1, 4.2km/s	--
PP-5 (P-2)	Velocity Thickness	--	0.5~0.6km/s 7.0m	1.2~1.3km/s 20m	2.1~2.2km/s 30m	4.1, 4.2km/s	--
PP-6 (P-1)	Velocity Thickness	--	0.5~0.6km/s 10m	1.0~1.1km/s 30m	2.0~2.2km/s 18~41m	4.1km/s	--

- **Upstream Damsite**

PU-1 (PS-12): Left Bank

The geological structure of this prospecting traverse is divided into five layers based on velocity values.

The velocity of the first layer is 0.35 to 0.4 km/s. This layer is partially missing at the first half of the traverse (near base of slope). The thickness of the layer increases near the end point (upper part of slope) and becomes 5.0 m at maximum.

The velocity of the second layer is 0.8 to 0.85 km/s. The layer thickness is 0.5 to 10 m, being extremely thin near the beginning point of the traverse and becoming increasingly thicker toward the ending point.

The velocity of the third layer is 1.3 to 1.4 km/s. This layer is missing near the beginning point of the traverse. Whereas the layer thickness is approximately 7 m at the first half of the traverse, it becomes thicker at the second half and 21 m at maximum.

The velocity of the fourth layer is 2.3 to 2.4 km/s. The layer thickness is 4.0 to 36 m, being thin near the beginning point of the traverse and thicker towards the ending point.

The fifth layer comprises the basement of this traverse and the velocity is 4.4 km/s.

PU-2 (PS-11): Left Bank (on Dam Axis)

The geological structure of this prospecting traverse is divided into five layers based on velocity values.

The velocity of the first layer is 0.25 to 0.35 km/s. This layer is missing in the vicinity of the beginning point of the traverse (on the base of the slope). The layer thickness becomes greater near the

ending point of the traverse (on the upper part of the slope) and becomes 5.0 m at maximum.

The velocity of the second layer is 0.6 to 0.7 km/s. The layer thickness is 4.0 to 13 m, and compared with the first half of the traverse, the second half is thicker.

The velocity of the third layer is 1.2 to 1.3 km/s. The layer thickness is extremely thin near the beginning point of the traverse, with the thickness becoming greater toward the ending point. The maximum layer thickness is 25 m.

The velocity of the fourth layer is 2.2 to 2.4 km/s. The layer thickness, other than becoming small at the vicinity of the beginning point at 6.0 m, is more or less uniform at approximately 20 m. The maximum layer thickness is 25 m.

The fifth layer is the basement of this traverse and the velocity is 4.6 km/s.

PU-3 (PS-10): Left Bank

The geological structure of this prospecting traverse is divided into five layers based on velocity values.

The velocity of the first layer is 0.35 to 0.4 km/s. This layer is missing near the beginning point of the traverse (on the base of the slope). The layer thickness, other than becoming a maximum of 7.0 m in the vicinity of the ending point of the traverse (on the upper part of the slope) is more or less uniform at approximately 2 m.

The velocity of the second layer is 0.6 to 0.7 km/s. The layer thickness is 1.0 to 9.0 m with the latter half of the traverse becoming thicker compared with the first half.

The velocity of the third layer is 1.2 km/s. The layer thickness is extremely small near the beginning point of the traverse, becoming thicker toward the ending point. The maximum layer thickness is 23 m.

The velocity of the fourth layer is 2.2 to 2.3 km/s. The layer thickness, other than being thin at 4.5 m near the beginning point of the traverse, is more or less uniform and approximately 20 m. The maximum layer thickness is 26 m.

The fifth layer comprises the basement of this traverse and the velocity is 4.6 km/s.

PU-4 (PS-9): Right Bank

The geological structure of this prospecting traverse is divided into five layers based on velocity values.

The velocity of the first layer is 0.2 to 0.3 km/s. This layer is partially missing at the base of the slope which makes up the first half of the traverse. The layer thickness, other than being thin at approximately 0.5 m at the level plane near the beginning point of the traverse, is more or less uniform at approximately 2 m. The maximum layer thickness is 3.0 m.

The velocity of the second layer is 0.5 to 0.6 km/s. This layer is missing at the level plane previously mentioned. The layer thickness other than being thin at approximately 2 m near Receiving Point No. 50, is more or less uniform at approximately 4 m. The maximum layer thickness is 6.0 m.

The velocity of the third layer is 1.0 to 1.2 km/s. The layer thickness is small and approximately 4 m at the level plane, but becomes thicker at the slope. The maximum layer thickness is the 17 m at the middle of the slope.

The velocity of the fourth layer is 2.0 to 2.1 km/s. The layer thickness is 8.5 to 32 m, thin near the beginning point of the traverse and becoming thicker going toward the ending point.

The fifth layer comprises the basement of this traverse and the velocity is 4.6 km/s.

PU-5 (PS-8): Right Bank (On Center Line of Spillway)

The geological structure of this prospecting traverse may be divided into five layers based on velocity values.

The velocity of the first layer is 0.2 km/s. This layer is distributed only near the top of the slope making up the vicinity of the ending point of the traverse. The layer thickness is 1 to 2 m.

The velocity of the second layer is 0.45 to 0.6 km/s. This layer is partially missing at the level plane making up the first half of the traverse. The layer thickness, in contrast to it being thin at 1 to 2 m at the level plane, becomes thick for an average 5 m at the slope making up the latter half of the traverse. The maximum layer thickness is 8.5 m.

The velocity of the third layer is 0.9 to 1.0 km/s. The layer thickness is 2.0 to 21 m, and similarly to the second layer, it is thin at the level plane, becoming thicker at the slope.

The velocity of the fourth layer is 2.0 to 2.4 km/s, and there is a trend for lower velocity going from the level plane toward the slope. The layer thickness is 6.0 to 27 m, and similarly to the overlying layers, it is thin at the level plane and thicker at the slope.

The fifth layer comprises the basement of this traverse. The velocity, with the zone of low velocity distributed at roughly the middle of the traverse as the boundary, is 4.9 km/s on the beginning point side and 4.6 km/s on the ending point side. The velocity and width of the low-velocity zone are 2.4 km/s and 20 m respectively.

PU-6 (PS-9): Left Bank

The geological structure of this prospecting traverse is divided into five layers based on velocity values.

The velocity of the first layer is 0.15 to 0.3 km/s. This layer is distributed at the slope making up the vicinity of the beginning point of the traverse and the slope and the top of the slope making up the latter half of the traverse, but is missing at the river bed. The maximum layer thickness is 1.5 m.

The velocity of the second layer is 0.6 km/s. The layer thickness is 1.5 to 5.5 m, being thick at the middle part of the traverse and thinner at the two ends.

The velocity of the third layer is 1.2 km/s. This layer is distributed only at the top of the slope at the latter half of the traverse. The maximum layer thickness is 8.0 m.

The velocity of the fourth layer is 2.2 km/s. The layer thickness is more or less uniform and approximately 13 m.

The fifth layer comprises the basement of this traverse and the velocity is 4.4 km/s. It is estimated that there exists a low-velocity zone of velocity 2.5 km/s. and width 22 m at roughly the middle of the traverse.

- **Downstream Damsite**

PL-1 (PS-1): Right Bank

The geological structure of this prospecting traverse is divided into five layers based on velocity values.

The velocity of the first layer is 0.15 to 0.25 km/s. This layer is mainly distributed at the middle part of the traverse and is partially

missing near the two ends of the traverse. The maximum layer thickness is 3.0 m.

The velocity of the second layer is 0.5 to 0.6 km/s. The layer thickness is 1.0 to 11 m, thick at the middle part of the traverse, and thinner at the two end portions.

The velocity of the third layer is 1.2 to 1.3 km/s. The layer thickness is more or less uniform and approximately 12 m.

The velocity of the fourth layer is 2.1 km/s. The layer thickness is 22 to 42 m, with a slight tendency to become thicker where the topography is of convex form.

The fifth layer is the basement of the traverse and the velocity is 3.6 km/s.

PL-2 (PS-2): Right Bank (on Dam Axis)

The geological structure of this prospecting traverse may be divided into five layers based on velocity values.

The velocity of the first layer is 0.15 km/s. This layer is partially distributed at the first half of the traverse. The maximum layer thickness is 2.0 m.

The velocity of the second layer is 0.5 km/s. This layer is partially missing near the ending point of the traverse. The maximum layer thickness is 3.0 m.

The velocity of the third layer is 1.0 to 1.3 km/s, with it being higher the nearer the beginning point of the traverse. The layer thickness, other than being a minimum of 3.0 m in the vicinity of the ending point of the traverse, is more or less uniform and approximately 13 m. The maximum layer thickness is 17 m.

The velocity of the fourth layer is 2.0 to 2.2 km. The layer thickness is 17 to 36 m, being a maximum near the beginning point of the traverse and becoming thinner going toward the end point.

The fifth layer comprises the basement of the traverse and the velocity is 3.8 km/s.

PL-3 (PS-3): Right Bank

The geological structure of this prospecting traverse may be divided into five layers based on velocity values.

The velocity of the first layer is 0.2 km/s. This layer is distributed only at the latter half of the traverse and the maximum layer thickness is 1.5 m.

The velocity of the second layer is 0.4 to 0.6 km/s, and is higher the nearer the end point of the traverse. The layer thickness is 0.5 to 4.0 m.

The velocity of the third layer is 1.1 to 1.2 km/s. The layer thickness, other than being a minimum of 3.0 m in the vicinity of the ending point of the traverse, is more or less uniform at approximately 8 m. The maximum layer thickness is 10 m.

The velocity of the fourth layer is 2.0 to 2.1 km/s. The layer thickness is 12 to 27 m and is a maximum near the beginning point of the traverse, becoming thinner going toward the ending point.

The fifth layer comprises the basement of the traverse and the velocity is 3.8 km/s.

PL-4 (PS-4): Right Bank

The geological structure of this prospecting traverse is divided into five layers based on velocity values.

The velocity of the first layer is 0.3 to 0.35 km/s. This layer is distributed on the downstream side slope (on the ending point side of the traverse), and is missing on the upstream side slope and the ridge portion. The maximum layer thickness is 3.0 m.

The velocity of the second layer is 0.5 km/s at the upstream side slope (on the beginning point side of the traverse), and is 0.7 km/s at the downstream side slope. The layer thickness is greater at the downstream side slope compared with the upstream side slope. The maximum layer thickness is 7.0 m.

The velocity of the third layer is 1.2 to 1.3 km/s. The layer thickness is a maximum of 17 m at the ridge portion, and becomes thinner toward the bases of the slopes.

The velocity of the fourth layer is 2.2 to 2.4 km/s. The layer thickness is a maximum of 17 m at the ridge portion, and becomes thinner toward the bases of the slopes.

The fifth layer comprises the basement of this traverse. The velocity is 4.4 km/s at the downstream side slope, while it is estimated to be 3.8 km/s from the intersecting traverses with regard to the upstream side slope and the ridge portion.

PL-5 (PS-6): Right Bank

The geological structures of this prospecting traverse is divided into five layers based on velocity values.

The velocity of the first layer is 0.25 to 0.3 km/s. This layer is partially missing at the base of the upstream side slope (on the beginning point side of the traverse) and a part of the downstream side slope. The maximum layer thickness is 4.0 m.

The velocity of the second layer is 0.6 to 0.7 km/s. The layer thickness is 1.5 to 5.0 m, being comparatively thick at mid-height of the downstream side slope.

The velocity of the third layer is 1.2 to 1.3 km/s. The layer thickness is a maximum of 13 m at the ridge portion, and a minimum of 2.5 m at the base of the upstream side slope. The layer thickness of the downstream slope is more or less uniform and approximately 9 m.

The velocity of the fourth layer is 2.0 to 2.2 km/s. The layer thickness is 4.5 to 32 m, being a maximum at the ridge portion and becoming thinner going toward the bases of the two slopes.

The fifth layer comprises the basement of this traverse. The velocity is 4.2 km/s at the downstream side slope, while it is estimated to be 3.8 km/s from intersecting traverses with regard to the ridge portion and the upstream side slope. It is estimated there exists a low-velocity zone of velocity 2.7 km/s and width 34 m at roughly the middle of the downstream side slope.

PL-6 (PS-1): Left Bank

The geological structure of this prospecting traverse is divided into three layers based on velocity values. The velocity layer corresponding to the second layer of other traverses is not distributed at this traverse. Furthermore, it is surmised that the basement corresponding to the fifth layer was not detected because of the shortness of the traverse length.

The velocity of the first layer is 0.4 km/s. This layer is distributed only at the latter half of the traverse. The maximum layer thickness is 1.5 m.

The velocity of the third layer is 1.1 km/s. This layer is exposed at the ground surface at the first half of the traverse. The layer thickness is 2.5 to 5.0 m, and compared with the first half, the latter half is slightly thicker.

The fourth layer is the apparent basement of this traverse and its velocity is 1.7 km/s.

- **Power Station Site**

PP-1 (P-7): Upper Penstock Route

The geological structure of this prospecting traverse is divided into five layers based on velocity values.

The velocity of the first layer is 0.3 to 0.35 km/s. This layer is missing at depressions in the topography and at parts of the slope. The layer thickness is especially thick in the vicinity of the traverse ending point and reaches 11 m at maximum.

The velocity of the second layer is 0.6 to 0.7 km/s. This layer is partially missing at a part of the first half of the traverse (Receiving Points Nos. 26 to 41). Other than the layer thickness becoming the maximum 9.0 m in the vicinity of the ending point of the traverse, the layer thickness is more or less 2 to 3 m.

The velocity of the third layer is 1.1 to 1.4 km/s. This layer is missing at the depression (Receiving Point No. 91) existing at the latter half of the traverse. The layer thickness, other than being especially large at 28 m near the end point of the traverse, is more or less uniform at approximately 14 m.

The velocity of the fourth layer is 2.0 to 2.4 km/s. The layer thickness is from 17 to 58 m, thinner at the first half of the traverse and thicker at the second half. The zone of low velocity distributed from Receiving Points No. 16 to No. 31 comprises a part of a velocity layer continuous from an underlying low-velocity zone.

The fifth layer comprises the basement of this traverse. Velocities differ bounded by two low-velocity zones distributed in the basement, the middle portion sandwiched by low-velocity zones being 4.0 to 4.1 km/s, and outer parts of low-velocity being respectively 3.4 km/s. The low-velocity zones are distributed from Receiving Points No. 16 to No. 32 and from No. 81 to No. 85, the velocities and widths being 2.2 km/s and 155 m, and 2.6 km/s and 40 m, respectively.

PP-2 (P-5): Lower Penstock Route and Power Station Site

The geological structure of this traverse is divided into five layers based on velocity values.

The velocity of the first layer is 0.3 to 0.35 km/s. This layer is mainly distributed at the latter half of the prospecting line, and elsewhere, is only distributed fragmentarily. The maximum layer thickness is 5.0 m.

The velocity of the second layer is 0.6 to 0.7 km/s. This layer is missing in the vicinity of the beginning point (on the terrace cliff) of the traverse. The layer thickness is more or less in a range of 3 to 8 m.

The velocity of the third layer is 1.0 to 1.2 km/s, and is highest near the starting point (on the terrace plane) of the traverse. This layer is missing in the vicinity of the river bed. The layer thickness is large at the terrace plane and small at the middle portion of the traverse. The maximum layer thickness is 25 m.

The velocity of the fourth layer is 2.0 to 2.3 km/s. The layer thickness is 10 to 30 m, and it is estimated that the thickness is smaller at the edge of the riverbed.

The fifth layer comprises the basement of the traverse. The velocity is 3.7 to 4.0 km/s on the beginning point side of the traverse and 3.4 km/s on the end point side with a low-velocity zone distributed from Receiving Points No. 137 to No. 143 as the boundary. The velocity and width of the low-velocity zone are 2.2 km/s and 60 m, respectively.

PP-3 (P-3): Power Station Site

The geological structure of this prospecting traverse is divided into four layers based on velocity values. The velocity layer corresponding to the first layers at other traverses is missing. The

first layers of PP-4 to PP-6 laid out at the power station site are similarly missing. The individual velocity layers are described below beginning with the second layer which is the top layer.

The velocity of the second layer is 0.5 to 0.65 km/s. The layer thickness is 1.0 to 4.0 m, being thick at the middle portion of the traverse line and thinner near both ends.

The velocity of the third layer is 1.1 to 1.4 km/s, being higher the close to the ending point of the traverse. The layer thickness is more or less uniform and approximately 16 m.

The velocity of the fourth layer is 2.0 to 2.1 km/s. The layer thickness is 22 to 45 m, being thin in the vicinity of the intersection with PP-2 and in the vicinity of the end point of the traverse.

The fifth layer comprises the basement of the traverse and the velocity is 4.1 km/s.

PP-4 (P-4): Power Station Site

The velocity of the second layer is 0.4 to 0.5 km/s. This layer shows a fragmentary distribution mode and is mostly missing at depressions in the topography. The maximum layer thickness is 4 m.

The velocity of the third layer is 1.1 to 1.2 km/s. This layer is missing at the end point of the traverse. The layer thickness is roughly uniform except for the vicinity of the prospecting line ending point and is approximately 18 m.

The velocity of the fourth layer is 2.0 to 2.3 km/s. The layer thickness, whereas it is 5 to 10 m near the ending point of the traverse, is thick elsewhere, being from 20 to 25 m.

The fifth layer comprises the basement of this traverse, and the velocity is 4.1 to 4.2 km/s.

PP-5 (P-5): Power Station Site

The geological structure of this traverse is divided into four layers based on velocity values.

The velocity of the second layer is 0.5 to 0.6 km/s. This layer is missing in the vicinity of the river bed (at the starting point of the traverse). The thickness of the layer, contrasted to being 4 to 6 m on the terrace plane, is less than 2 m at the slope near the end point of the traverse.

The velocity of the third layer is 1.2 to 1.3 km/s. The layer thickness, contrasted to being 3 to 8 m in the vicinity of the riverbed, is more or less uniform elsewhere and approximately 18 m. The maximum layer thickness is 20 m.

The velocity of the fourth layer is 2.1 to 2.2 km/s. The layer thickness is 6 to 10 m near the riverbed, and more or less uniform at the terrace plane and approximately 24 m, becoming slightly thick at the slope and approximately 30 m.

The fifth layer comprises the basement of this traverse, and its velocity is 4.1 to 4.2 km/s.

PP-6 (P-1): Power Station Site

The geological structure of this prospecting traverse is divided into four layers based on velocity values.

The velocity of the second layer is 0.5 to 0.6 km/s. This layer is missing in the vicinity of the river bed (on the beginning point of the traverse). The layer thickness, other than being a maximum of 10 m near the ending point of the traverse, is more or less 5 m.

The velocity of the third layer is 1.0 to 1.1 km/s. The layer thickness is 3 to 10 m at the first half of the traverse, whereas it is 20 to 30 m at the latter half.

The velocity of the fourth layer is 2.1 to 2.2 km/s. The layer thickness, other than being thin in the vicinity of the riverbed and between Receiving Points No. 20 and No. 25 at 20 to 25 m, is more or less 30 to 40 m.

The fifth layer comprises the basement of the traverse, and its velocity is 4.1 km/s.

(2) In-Adit Seismic Prospecting

According to the result of seismic prospecting in Adit UA-1 located at the upper damsite, level of velocity is generally lower than that of surface seismic prospecting, and the velocity is as slow as 1.5 km/s even at the 40 m or inner from the portal.

This originates in that the rock mass around the adit has been much loosened during excavation. The fact indicates that the rock mass is apt to be loosened by dynamite excavation as compared to that of lower damsite, as explained later.

The velocity is as follows:

- LA-1: Portal - 7.5 m : 1.7 km/s or less
7.5 m or inner : 2.9 km/s ~ 4.8 km/s
- LA-2: Portal - 31.0 m : 1.7 km/s or less
31.0 m or inner : 2.8 km/s ~ 3.9 km/s

The result indicates that the rock mass is rather loosened from surface to the depth at the right bank than the left bank.

The time-distance plots and analysis diagrams of in-adit seismic prospecting performed inside adits at three locations are shown in Appendix A-5-6. The rock masses in the adits were divided into four to five velocity zones based on analysis results. The results of the investigations are given in Table 7-18.

**Table 7-18 Seismic Velocity Distribution
in Adits of the Pirris Damsites**

Adit No.	Distance (m)	Seismic Velocity (km/s)	Remarks
PUA-1	0 ~ 5.0	0.6	On the left bank of up-stream damsite
	5.0 ~ 40.0	1.1	
	40.0 ~ 50.0	1.5	
PLA-1	0 ~ 7.5	1.7	On the left bank of down-stream damsite
	7.5 ~ 17.5	2.9	
	17.5 ~ 37.5	4.8	
	37.5 ~ 50.0	3.1	
PLA-2	0 ~ 10.5	1.1	On the right bank of down-stream damsite
	10.5 ~ 31.0	1.7	
	31.0 ~ 42.5	3.9	
	42.5 ~ 50.0	2.8	

7.9 Construction Materials

7.9.1 Construction Materials and Tests

Regarding investigations and tests of construction materials, surface explorations at candidate sites were carried out by the JICA Survey Team and ICE, and laboratory tests were conducted on samples obtained from the various sites by the ICE.

The laboratory tests were carried out on concrete aggregates, boring cores, rock materials, and soil materials. Of these, the drilling core tests include obtaining of foundation rock strength and their results are explained in 7.10. The locations of sites where samples of concrete aggregates, drilling cores, rock materials, and soil materials were collected are shown in Fig. 7-17. The test quantities and test items concerning the samples collected are given in Table 7-19.

In regard to concrete aggregate samples, since there was no place where natural aggregates such as river deposits could be collected as shown in Fig. 7-17, samples were collected from the two locations of the right-bank side mountain mass sandstone formation at the proposed upstream damsite as a prospective site for a quarry site (including UB-2, UB-3) to collect raw rock for crushed stone aggregates, and inside the LA-2 exploratory adit in the right-bank side mountain mass of dolerite-basalt at the proposed downstream damsite.

Samples of drilling core tests were collected from drilling cores from UB-1, UB-2, and UB-3 located in the sandstone formation at the upstream damsite and LB-1, LB-2, LB-3, and LB-4 located in the dolerite-basalt of the right-bank mountain mass at the downstream damsite.

Samples of rock materials and filter materials were collected inside the exploratory adit LA-2 in dolerite-basalt distributed at the downstream damsite taking into consideration the case of a rockfill dam being selected as the type of dam for this Project.

Soil (core) materials samples were collected from test pits CP-1, CP-2, and CP-3 at talus deposits on the right-bank slope approximately 2 km upstream of the upstream damsite.

The data of laboratory tests performed by ICE are given in Appendix A-6.

7.9.2 Concrete Aggregates

A summarization of the results of concrete aggregate tests is contained in Table 7-20. Evaluations of these results are given below.

- (1) The specific gravities of the sandstone of the upstream damsite and the dolerite-basalt of the right bank-side mountain mass at the downstream damsite are from 2.49 to 2.93, and these values are in the standard range for concrete aggregates.
- (2) Absorption rates are from 0.50 to 5.1% but the majority of the values is in the general range of 0.3 to 3.0% for aggregates and there will be no problem.
- (3) Soundness test values are from 2.4 to 9.5%, and being under 10%, there will be no problem.
- (4) Abrasion resistance in the Class A particle size division (10 to 40 mm) is low at 14.7 to 16.4%, adequately below 40% for good resistance.
- (5) There is little weight reduction of samples in durability tests, and the Slake Durability Index is high from 97.2 to 98.7% to indicate good quality.
- (6) Alkali-aggregate reaction tests were conducted by the chemical method, and as indicated in the reactivity judgment chart (Appendix A-6) there will be no problem.
- (7) The particle-size distributions after crushing once in the crushed stone tests, show aggregates to be in the ranges for standard gradations, 40

to 5 mm for coarse aggregate and under 5 mm for fine aggregate, indicating good gradations.

However, when evaluated based on values after having crushed twice, there is a tendency seen in the test results for slightly excessive fine division.

Regarding particle shapes, there is a slight tendency for flat shapes with flatness 0.44. And, slenderness is 1.86 for a shape on the slender side. Since it is said unit water content will be lower and workability better the more that aggregate particle shape is close to being spherical, it may be said aggregates will be of good quality the more that both flatness and slenderness are close to 1.0.

- (8) The rocks are sound with ultrasonic wave velocities from 5.25 to 5.57 km/sec, moduli of elasticity from 236,000 to 272,000 kg/cm², compressive strength from 694 to 1,530 kg/cm², and therefore, sufficient strengths for concrete aggregates.
- (9) The interrelationships of the various test results also are in good agreement with general values. For example, there are relationships between specific gravity and absorption, absorption and soundness, absorption and abrasion loss, specific gravity and compressive strength, and absorption and compressive strength, and that these relationships are in comparatively good agreement indicates that it may be said the reliability as test result is good.

As a whole, the sandstone formation of the mountain mass at the right-bank side of the upstream damsite, and the dolerite-basalt in the exploratory adit LA-2 in the mountain mass at the right-bank side of the downstream damsite, and samples collected from them are good quality as concrete aggregates, and are materials which can be used.

It is thought necessary hereafter to grasp in detail the overall concrete volume required, and calculate the amount of concrete aggregates required for this volume, along with which more detailed investigations must be made of the

amounts of material which can be collected from the proposed quarry sites, and investigations and tests carried out concerning artificially crushed rock.

7.9.3 Rock Materials

Result of Rock material tests were considered on the tests with samples collected from inside the exploratory adit LA-2 in dolerite-basalt distributed at the downstream damsite, and the results of tests on boring core samples from LB-1, LB-2, LB-3, and LB-4 located in the dolerite-basalt at the right-bank side mountain mass at the downstream damsite. These test results are given in Tables 7-20 and 7-21, and the evaluations are as listed below.

- (1) Specific gravities are in a range from 2.80 to 2.93 and good.
- (2) Absorption rates are low at 0.58 to 1.70% and pose no problems.
- (3) Compressive strengths range from 856 to 1,530 kg/cm² and are good.
- (4) With regard to other qualities, deformability is from 230,000 to 272,000 kg/cm² in terms of modulus of elasticity, the percentage of loss in soundness tests is low at 2.4%, and the durability index is high at 98.7%, so that all properties are favorable.

Hence, this material is from heavy and dense rock mass, suitable as crude rock for rock material, while finer particles are suitable as filter material.

7.9.4 Soil Materials

Soil (core) material tests were performed on top soil from the right-bank slope approximately 2 km upstream of the upstream damsite, and samples collected from 3 test pits in talus deposits. The test results are given in Table 7-21 with evaluations as listed below.

- (1) Specific gravities are in a range of 2.68 to 2.73 and are good.

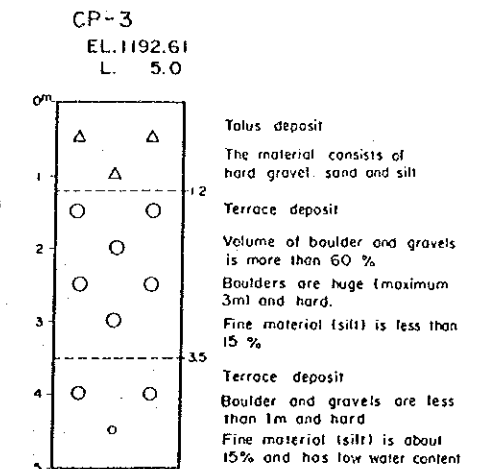
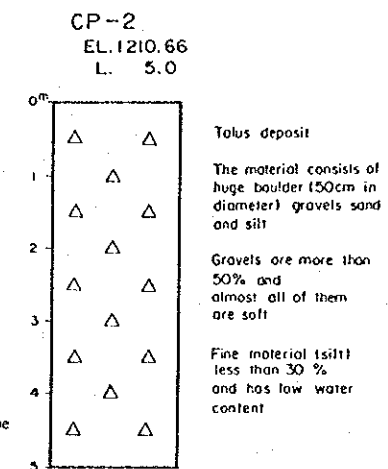
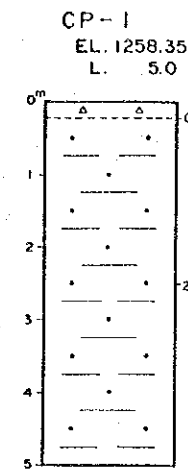
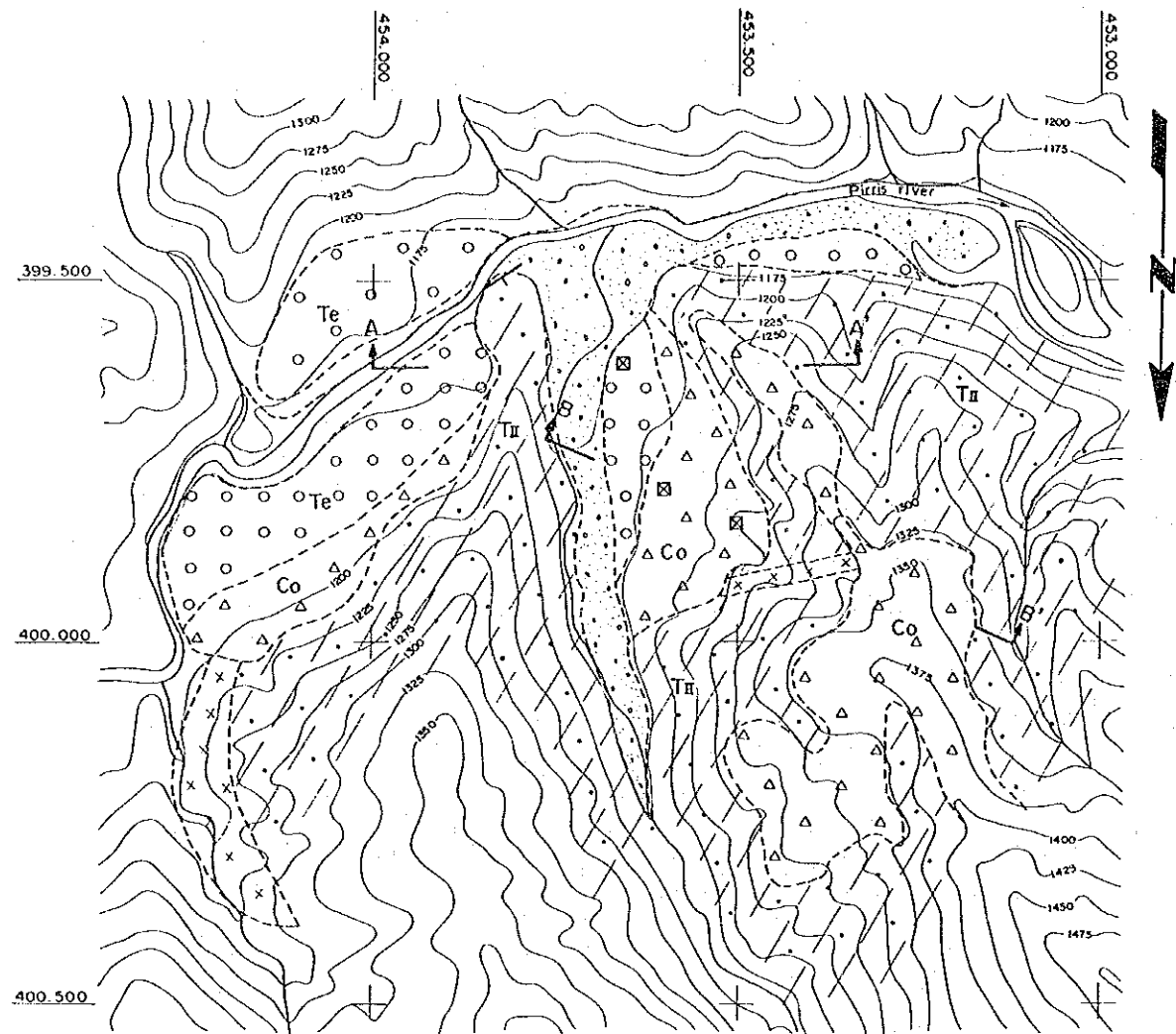
- (2) Natural water contents range from 23.0 to 30.8%, which are values for normal moist soil.

The optimum water content is in a range from 19.2 to 28.2%, a general range slightly lower than the natural water content.

- (3) The natural grain-size distribution is more or less satisfactory, and there will be no problem as it is in the standard grain-size distribution range for soil materials.
- (4) Liquid limits (LL) are 34 to 65%, distributed centering on Line B in the plasticity chart. Plasticity indices (PI) are in a range of 6 to 27% and distributed below Line A. The soil classification is mostly SM, with some MH and ML. The material of SM class is often used as soil materials (core material) for fill-type dams in general and is adequate.
- (5) The results of compaction tests were unit weights of 1.439 to 1.608 t/m³ at optimum water content so that some were on the somewhat light side, but mostly were 1.550 t/m³ or higher, and since it is thought they can be higher when compacting energy is considered, there will be no problem.
- (6) The results of permeability tests are 3.40 to 0.95 x 10⁻⁷ cm/sec and adequately below the required 10⁻⁵ cm/sec so that permeability is satisfactorily low.
- (7) In triaxial tests, CU tests (pore water pressure measured in consolidated and undrained state) were performed and the shear strength constants by the effective stress method were C of 0.4 to 1.2 kg/cm² and tan ϕ of 0.21 to 0.35. The tan ϕ values are slightly low and this is thought to be due to fine-grained soil contents of the samples being slightly high, and the contents of fine-particled gravel and sand being low.

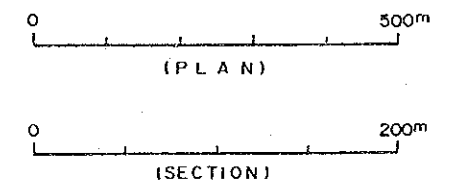
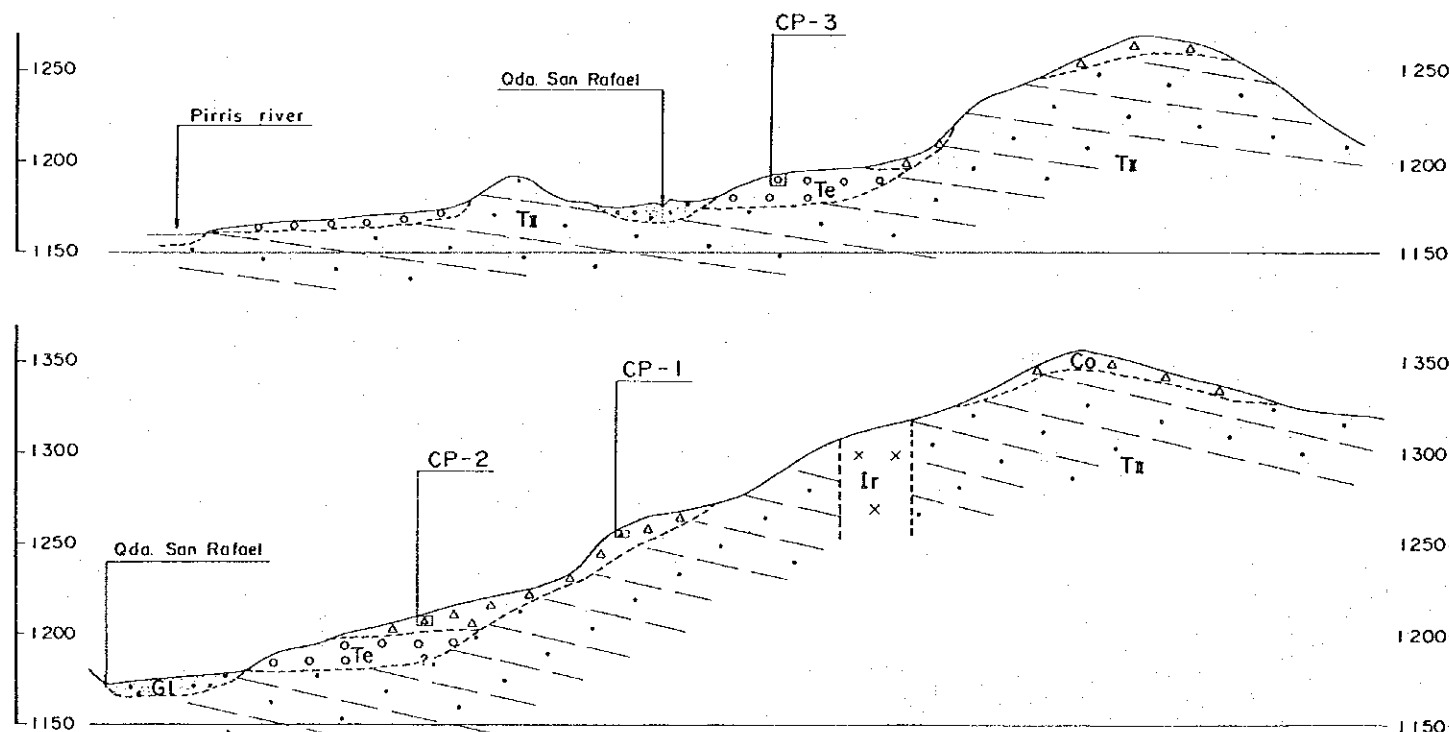
The foregoing are the results of tests on soil materials, and to summarize the overall characteristics, although plasticity index is slightly low and unit

weight slightly light, it is possible for this to be used as impervious material.



LEGEND

- River bed deposits
- Colluvial deposits (includes residual soil)
- Terrace deposits
- Sandstone with shale and conglomerate
- Intrusive rock
- Geologic boundary
- Test Pit
- Geologic section



REPUBLIC OF COSTA RICA
PIRRIS HYDROELECTRIC POWER
DEVELOPMENT PROJECT

GEOLOGY OF BORROW AREA

Fig.7-17 DATE:

Table 7-19 Quantity and Sampling Location of Laboratory Tests

Test Item	ASTM	Quantity	Sampling Location
1. Concrete Aggregate			
(1) Specific gravity and absorption	C 127-84	2	Quarry Site (Right Bank of Upstream Dam site) and Right Bank Adit of Downstream Dam site. (LA-2 Adit)
(2) Soundness test	C 128-84 C 88-83	2	
(3) Abrasion Loss Test	C 131-81	2	
(4) Slake Durability Test	D 4644-87	2	
(5) Alkali Aggregate Reaction Tests	C 289-81 C 227-81	2	
(6) Crushing Test	T. S-L. T	2	
2. Laboratory Test of Boring Core			
(1) Specific gravity, absorption Tests	C 127-84 C 128-84	7	UB-1, UB-2, UB-3 and LB-1, LB-2, LB-3, LB-4
(2) Ultrasonic Test	D 2845-83	7	
(3) Unconfined Compression Test	D 2938-79	7	
(4) Tensile Test	D 3967-81	7	
3. Rock Materiales			
(1) Specific gravity and absorption	C 127-84 C 128-84	1	Right Bank Adit of Downstream Dam site. (LA-2 Adit)
(2) Unconfined Compression Test	D 2938-79	1	
4. Soil Materiales			
(1) Specific gravity Test	C 127-84 D 854-83	4	CP-1, CP-2, CP-3 and CP-M (Mixture CP-1, -2, -3)
(2) Moisture Test	D 2216-80	4	
(3) Grain-size Analysis Test	D 422-63	4	
(4) Liquid Limit & Plastic Limit Test	D 4318	4	
(5) Compaction Test	D 698-78	4	
(6) Permeability Test	T. S-L. T	4	
(7) Triaxial Compression Test	T. S-L. T	4	

Table 7-20 Result of Concrete Aggregate and Drilling Core on Laboratory Tests

Sampling Location	Test Item	Specific Gravity	Absorption (%)	Soundness (%)		Abrasion Loss (A) (%)	Slake Durability (%)	Alkali Reaction	Crushing	Remarks	
				3.5 (Coarse) 9.5 (Fine)	2.4 (Coarse) 4.0 (Fine)						
1. Concrete Aggregate											
Quarry Site (Right bank of Upstream Dam site)		2.51 (Co)	3.7 (Co)		16.4	97.2		Innocuous	0.44 (FL) 1.86 (SL)	(Co= Coarse) (Fi= Fine) (FL= Flatness) (SL= Slender- ness)	
	LA-2 Adit (Right bank of Downstream Dam site)	2.80 (Co) 2.49 (Fi)	1.7 (Co) 5.1 (Fi)		14.7	98.7		Innocuous	---		
Sampling Location	Test Item	Specific Gravity	Absorption (%)	Ultrasonic			Modulus of Elasticity		Unconfined Compression Strength (kg/cm ²)	Tensile Strength (kg/cm ²)	Remarks
				Vp (km/sec)	Vs (km/sec)	Vp Vs (km/sec)	Dynamic (kg/cm ²)	Static (kg/cm ²)			
2. Laboratory Test of Boring Core											
UB-1 (Left bank of U. Dam site) UB-2 (Right bank of U. ' ' ') UB-3 (' ' ' of U. ' ' ')		2.71	0.50	5.25	3.00	468,000	250,000	781	---		
		2.70	0.76	5.31	2.92	433,000	236,000	694	---		
		2.72	0.93	---	---	---	---	942	---		
		2.87	1.25	5.36	2.99	484,000	261,000	856	80		
LB-1 (Left bank of D. Dam site) LB-2 (Right bank of D. ' ' ') LB-3 (' ' ' of D. ' ' ') LB-4 (' ' ' of D. ' ' ')		2.90	0.58	5.57	2.99	484,000	265,000	1,089	96		
		2.88	0.59	5.53	3.05	502,000	272,000	1,065	93		
		2.93	1.02	5.27	2.93	433,000	230,000	1,530	---		

Table 7-21 Result of Rock and Soil Materials on Laboratory Tests

Test Item	Specific Gravity	Absorption (%)			Unconfined Compression (kg/cm ²)						Remarks
		Grain-size Analysis	Liquid Limit	Plasticity Index	Compaction	Permeability	Triaxial Compression	Classification			
Sampling Location		-0.005 (mm)	-0.074 (mm)	-4.8 (mm)	LL (%)	PI (%)	(kg/m ³)	x10 ⁻⁶ (cm/sec)	C	ϕ	
3. Rock Materials											
LA-2 Adit (Right bank of Downstream Dam site)	2.88		1.03				1,135				
4. Soil Materials											
CP-1 (Right bank of Upstreamward)	2.73	16~31	65~79	73~90	46~65	19~27	1,439	0.095	0.40	19° 30'	MH
CP-2 (' of ')	2.68	8~14	37~52	75~95	34~38	6~11	1,608	0.340	1.12	13° 25'	SM
CP-3 (' of ')	2.68	4~11	17~36	27~69	34~38	6~11	1,590	-----	1.20	12° 00'	SM
CP-M (' of ')	-----	-----	-----	-----	-----	-----	1,550	-----	-----	-----	-----

7.10 Drilling Core Tests

Drilling core tests were carried out on the sandstone at the upstream damsite and the dolerite-basalt of the right-bank mountain mass at the downstream damsite.

The test results are as given in Table 7-20 and the evaluations are as follows:

Sandstone at Upstream Damsite (UB-1, UB-2, UB-3)

- (1) Specific gravities are from 2.70 to 2.72, and although slightly low compared with the dolerite basalt at the downstream damsite, it is heavy for sandstone and satisfactory.
- (2) Absorption is from 0.50 to 0.93%, comparatively low, but indicating good quality.
- (3) Ultrasonic wave velocity (V_p) is from 5.25 to 5.31 kg/sec, fast for sandstone, indicating density.
- (4) Static moduli of elasticity are from 236,000 to 250,000 kg/cm², which are general values.
- (5) Compressive strengths are in a range of 694 to 942 kg/cm², and strength of rock as a dam foundation is adequate.

Dolerite-Basalt at Downstream Damsite (LB-1, LB-2, LB-3, LB-4)

- (1) Specific gravities are from 2.83 to 2.90, which is heavy for dolerite-basalt and good.
- (2) Absorption rates are from 0.58 to 1.25%, comparatively low, which is good.
- (3) Ultrasonic wave velocities (V_p) are in a range of 5.27 to 5.57 kg/sec, which are velocities of a general level.

- (4) Static moduli of elasticity range from 230,000 to 272,000 kg/cm², which are somewhat low in general.
- (5) The range of compressive strengths is from 856 to 1,530 kg/cm² and broad, but there will be no problem since the strength of rock for a dam foundation is adequately possessed.
- (6) Tensile strengths are from 80 to 96 kg/cm², results which are stable and good.

To summarize the above results, the sandstone at the upstream proposed damsite and the rock of the dolerite-basalt bedrock at the downstream proposed damsite possess satisfying rock strengths for a dam foundation.

References

- (1) Mapa Geologico de Costa Rica (1/200,000), M.I.E.M. 1982
- (2) Estudio Geologico de Parte de la Cuenca Media del Rio Pirris, ICE, 1984
- (3) Informe Geotecnico Prelinar No. 1 Sitio de Presa y Tuberia de Presion Project Hidroelectrico Pirris, ICE, 1984
- (4) Manual del Geologia de Costa Rica, Volumen I Estratigrafia, Peter Sprechmann, Universidad de Costa Rica, 1984
- (5) Analisis Geologico-Geomorfologico de la Cuenca del Rio Pirris, ITC, 1985
- (6) Informe Final Mapa Geologico de Costa Rica (1/500,000), ICE, 1988

CHAPTER 8 SEISMICITY

CHAPTER 8 SEISMICITY

Contents

	<u>Page</u>
8.1 Seismicity in Costa Rica	8 - 1
8.1.1 Outline	8 - 1
8.1.2 Seismic Activity in and around Costa Rica	8 - 2
8.2 Seismic Evaluation for Pirris Project Site	8 - 4
8.2.1 Historical Earthquakes around Pirris Project Site	8 - 4
8.2.2 Seismic Risk Analysis based on Stochastic Technique	8 - 8
8.2.3 Maximum Acceleration estimated for Pirris Project Site	8 - 20
8.2.4 Design Horizontal Seismic Coefficient	8 - 21
8.3 Afterword	8 - 23

List of Figures

- Fig. 8-1 Seismo-tectonics in Central-South America
- Fig. 8-2 Seismicity around Costa Rica during 1904-1991
- Fig. 8-3 Historical Earthquakes in the Vicinity of Pirris Project Site
- Fig. 8-4 Seismic Risk Analysis Techniques
(Stochastic Technique and Deterministic Technique)
- Fig. 8-5 Return Period for Maximum Acceleration calculated by Eq. (1)
- Fig. 8-6 Return Period for Maximum Acceleration calculated by Eq. (2)
- Fig. 8-7 Return Period by Maximum Acceleration calculated by Eq. (3)
- Fig. 8-8 Return Period by Maximum Acceleration calculated by Eq. (4)
- Fig. 8-9 General Procedure of Earthquake Resistant Design for Dam

List of Tables

- Table 8-1 Recent Earthquake Disasters in Costa Rica
- Table 8-2 Seismicity in Pirris Project Area
($M \geq 5.5$, $D \leq 200$ km)
- Table 8-3 Historical Earthquakes in the Vicinity of Pirris Project Site
- Table 8-4 Annual Number of Earthquakes during 1904-1991
($D \leq 1,000$ km, D: Epicentral Distance)
- Table 8-5 Distribution of Magnitude and Epicentral Distance of Earthquakes during 1904-1991
- Table 8-6 Annual Maximum Accelerations during 1904-1991
- Table 8-7 Maximum Accelerations for Six Return Periods
- Table 8-8 Design Horizontal Seismic Coefficient for Dam

CHAPTER 8 SEISMICITY

8.1 Seismicity in Costa Rica

8.1.1 Outline

Costa Rica is located on the Circum-Pacific Seismic Belt, and has suffered earthquake disasters many times in the past. Recent typical cases of earthquake disaster are as given in Table 8-1.

Since Costa Rica is situated in a natural environment of high seismic activity in this way, it is essential that thorough evaluation be made regarding earthquakes and proper considerations be given in the earthquake resistant design of electric power facilities.

Here, the seismic risk analysis based on the stochastic technique is performed. And the maximum acceleration at the dam site which is absolutely necessary as a fundamental condition in carrying out the earthquake-resistant design is evaluated.

Table 8-1 Recent Earthquake Disasters in Costa Rica

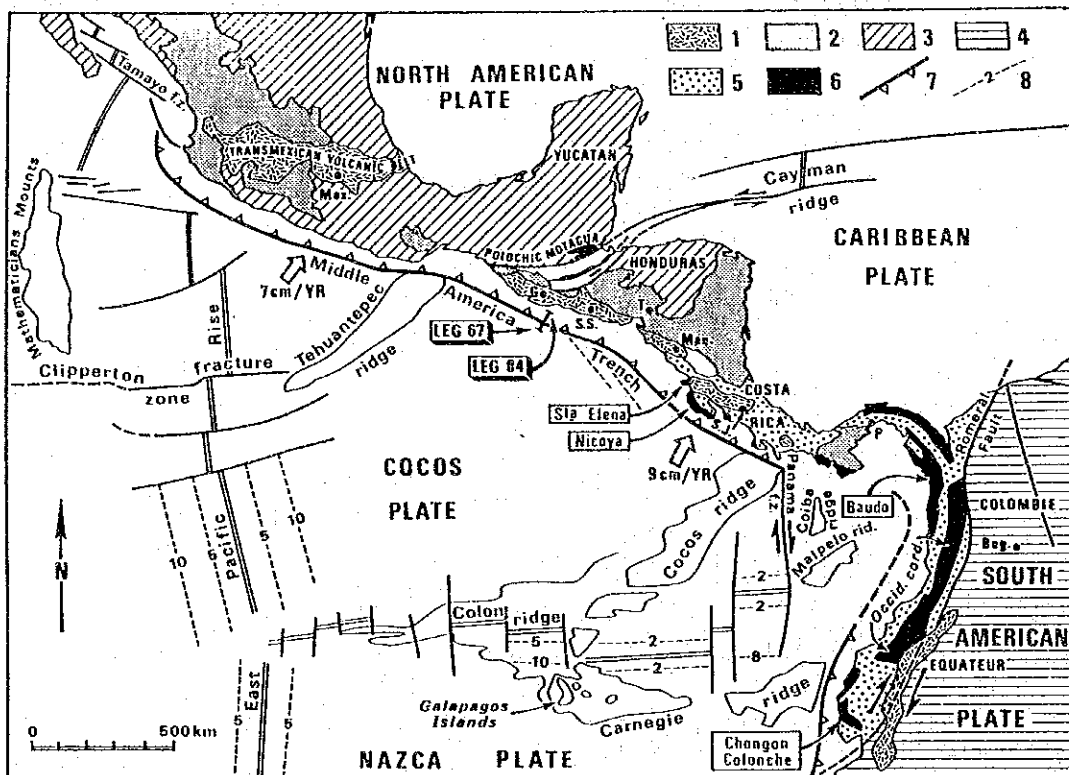
Earthquake Disaster			Damage		
Date	Type	Location	Killed	Affected	Homeless
04-14-73	Earthquake	S. of Laguna Arenal	21	3,563	84
			Comments: 98 Injured		
04-02-83	Earthquake	SE of San Jose	1	475	475
			Comments: 200 Injured		
07-03-83	Landslides (due to earthquake)	San Jose Province	1	5,000	0
04-22-91	Earthquake (MS=7.4)	SW of Limon (9°36.88'N 83°9.48'E)	48	6,840	6,752
			Comments: 585 Injured		

Source: OFDA Disaster History on file at the Office of U.S. Foreign Disaster Assistance in Washington, DC. Covers 1900 to the present.

8.1.2 Seismic Activity in and around Costa Rica

(1) Seismo-tectonics

The Central and South American regions from Mexico to Colombia, Ecuador, and Peru, as shown in Fig. 8-1, comprise a belt of seismic upheavals where the North American Plate, Pacific Plate, Cocos Plate, Caribbean Plate, Nazca Plate, and South American Plate collide against each other in complex manners. The region of Costa Rica on the side of the Pacific Ocean happens to be the boundary where the Cocos Plate sinks under the Caribbean Plate, and many earthquakes have occurred at this plate boundary in the past. Incidentally, the relative moving speed between the Cocos Plate and the Caribbean Plate is approximately 9 cm per year.



Tectonic setting of the Santa Elena and Nicoya Peninsulas (Costa Rica) and of Legs 67 and 84 off Guatemala. Present-day plate motions from Minster and Jordan (1978). 1 = Pliocene and Pleistocene volcanism; 2 = Oligocene and Miocene volcanism; 3 = North American plate; 4 = South American plate; 5 = Cenozoic formations of ophiolitic Andes and southern Central America; 6 = Mesozoic and Cenozoic ophiolitic complexes; 7 = subduction zones; 8 = magnetic anomalies.

Fig. 8-1 Seismo-tectonics in Central-South America

(2) Historical Earthquakes

The epicenters of earthquakes which occurred within a radius of 1,000 km from the Pirris project site during the period from 1900 to 1991 are shown in Fig. 8-2. As is clear from the figure, the earthquakes have occurred frequently in the Pacific Ocean coastal region along the plate boundary in the vicinity of Costa Rica.

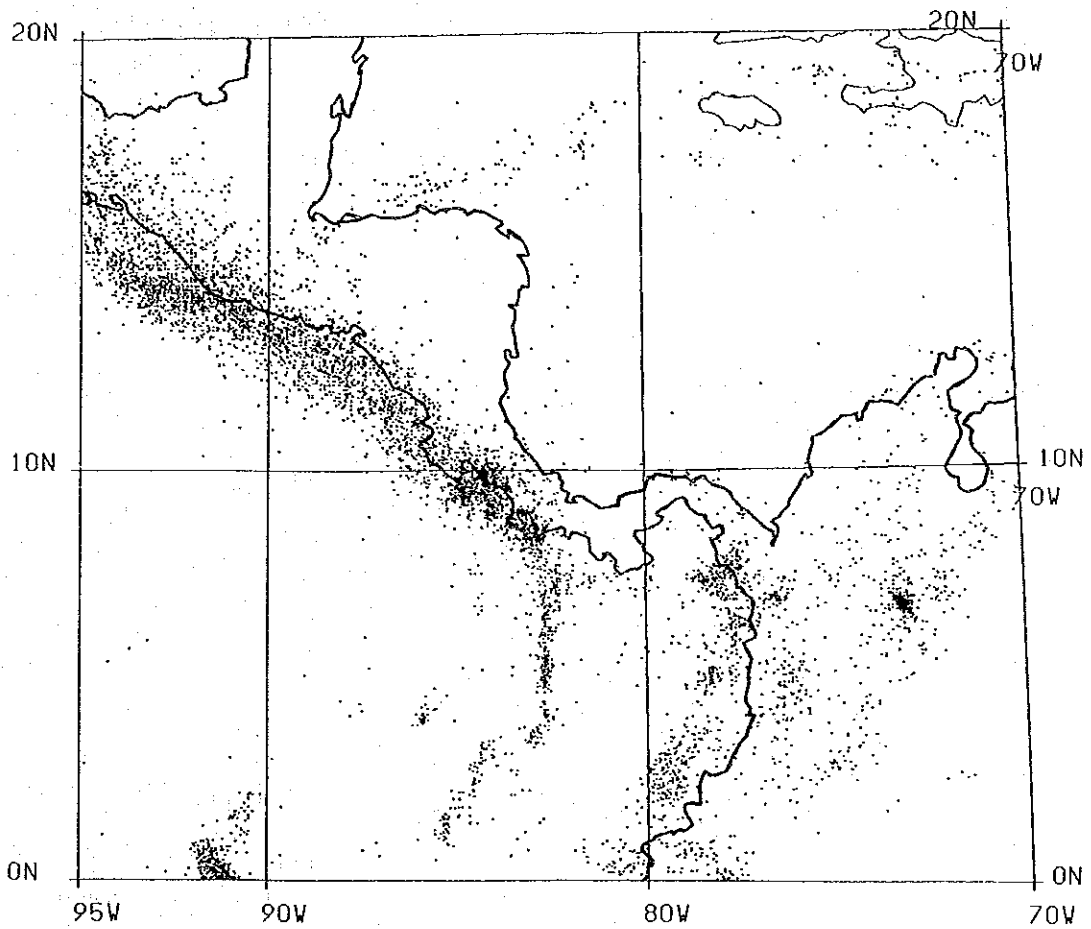


Fig. 8-2 Seismicity around Costa Rica during 1900-1991

8.2 Seismic Evaluation for Pirris Project Site

8.2.1 Historical Earthquakes around Pirris Project Site

A list of earthquakes of magnitude 5.5 or greater which have occurred within a radius of 200 km from the Pirris project site is given in Table 8-2. This table was made based on the historical earthquake events from the earthquake data files of the NOAA (National Oceanic and Atmospheric Administration) of the National Geophysical Data Center of the United States.

According to the table, the maximum magnitude of earthquakes which have occurred up to now in the surrounding area of Costa Rica was the M_L : 8.3 (local magnitude) [December 20, 1904 5hr 44 min 18 sec. focal depth: 60 km, epicentral distance: 77 km]. Of earthquakes of magnitude 5.5 or greater, the closest earthquake to the dam site occurred on March 4, 1924 (10hr 7min 42sec), which had an epicentral distance of 14 km (epicenter: Lat. 9.7°N , Long. 84.0°W , M_L : 7.0).

Further, the historical earthquakes occurring at the Pirris project site investigated by Instituto Costarricense Electricidad (ICE) are shown in Table 8-3 and Fig. 8-3.

In this investigation, the earthquakes which had occurred roughly within a radius of 90 km from the project site were picked up. According to the results of this investigation, the maximum magnitude of earthquakes which have occurred in the neighborhood of the Pirris project site was the M_s : 7.3 (surface wave magnitude) [(1) April 24, 1916, epicentral distance : 73 km, (2) December 21, 1939, epicentral distance : 70 km]. The earthquake which occurred closest to the site was that of an epicentral distance of 27 km (April 13, 1910, $M = 5.2$). In Table 8-3, the modes of earthquakes are classified into two types. One is the plate boundary earthquakes, and the other is the inland earthquakes. The plate boundary earthquakes occurred at the plate boundaries. The inland earthquakes occurred in inland areas. From the table, it may be comprehended that the earthquakes in excess of magnitude 7.0 were all plate boundary earthquakes (notation: S).

Table 8-2 Seismicity in Pirris Project Area

$M \geq 5.5, D \leq 200$ km

Date					Epicenter		Magnitude		H	D	R	
year	month	day	Time		N. Lat.	Long. W	M_b	M_L	(km)	(km)	(km)	
1904	12	20	5	44	18	8.50	83.00	7.7	8.3	25	177	178
1909	08	16	6	58	00	10.00	84.30	7.0	7.1	60	44	74
1916	04	24	8	02	08	11.00	85.00	7.3	7.6	60	178	188
1916	04	24	8	02	12	11.00	85.00	7.1	7.3	30	178	180
1916	04	26	2	21	30	10.00	85.00	7.1	7.3	30	104	108
1924	03	04	10	07	42	9.70	94.00	6.9	7.0	30	14	33
1931	12	20	14	59	42	11.00	94.50	6.1	5.7	280	155	320
1936	03	20	18	46	28	11.00	84.00	6.0	5.6	30	150	152
1937	03	09	15	40	20	9.00	83.50	6.5	6.4	30	99	103
1939	06	18	16	46	05	10.00	83.00	6.6	6.5	70	128	146
1939	12	21	20	54	48	10.00	85.00	7.1	7.3	30	104	108
1939	12	22	4	44	00	10.00	84.50	6.8	6.7	30	57	64
1940	10	05	14	38	43	9.50	84.20	6.4	6.2	30	19	35
1940	10	27	5	35	37	9.70	84.50	6.8	6.7	30	42	52
1941	12	05	20	46	58	8.50	83.00	7.2	7.5	30	177	179
1941	12	06	1	25	01	10.50	85.20	6.3	6.0	30	151	154
1941	12	06	21	24	40	8.50	94.00	6.8	6.9	30	128	131
1948	11	19	1	04	24	10.00	83.50	6.9	7.0	80	78	112
1949	08	18	13	33	25	8.50	83.00	6.6	6.5	30	177	179
1950	10	05	16	09	31	11.00	85.00	7.4	7.7	30	178	180
1950	11	11	13	51	10	10.40	85.70	7.4	5.7	30	192	194
1952	04	25	6	02	00	8.10	83.20	6.1	6.3	30	199	201
1952	05	13	19	31	45	10.30	85.30	6.5	6.9	64	148	162
1952	09	09	12	54	42	9.20	84.20	6.8	6.8	30	51	59
1956	07	19	23	26	25	9.50	84.50	6.8	6.0	30	45	54
1957	04	08	20	18	09	8.50	83.00	6.3	6.5	30	177	179
1958	04	15	3	52	35	8.00	84.50	6.7	6.7	30	187	190
1958	06	06	9	11	14	8.00	84.50	6.8	6.6	30	187	190
1961	05	23	3	40	24	9.80	84.00	5.9	5.3	93	21	95
1966	03	27	18	53	41	8.80	83.50	5.9	5.7	41	116	123
1966	04	09	2	42	11	9.50	84.10	5.7	5.6	49	17	52
1972	02	07	19	14	47	8.54	83.87	5.5	5.9	14	125	126
1973	04	14	8	34	00	10.67	84.75	5.7	6.5	33	134	138
1974	02	28	20	20	10	9.33	84.06	5.8	6.2	46	35	58
1976	12	20	10	18	56	9.27	83.93	5.5	5.1	66	47	81
1978	08	23	38	32	2	10.20	85.22	5.7	7.2	56	136	147
1979	07	01	20	38	04	8.31	82.94	5.5	6.7	28	196	198
1979	08	24	4	26	54	8.95	83.48	6.1	6.5	40	104	111
1983	04	03	2	50	01	8.71	83.12	6.5	7.2	37	150	155
1983	04	03	3	04	13	8.65	83.32	5.5	5.1	33	140	144
1983	07	03	17	14	23	9.65	83.68	5.9	6.7	33	47	57
1983	09	23	23	44	30	8.42	83.39	5.6	5.2	42	158	163
1988	03	02	07	13	19	9.53	84.86	5.5	5.1	31	83	88
1988	03	11	03	44	56	8.88	83.11	5.7	5.4	51	138	147
1990	03	25	13	22	55	9.58	84.93	6.5	6.5	24	89	92
1990	03	25	13	16	05	9.55	84.95	5.7	5.4	23	92	94
1990	04	27	01	23	09	8.66	83.65	5.7	5.4	24	120	122
1990	04	28	01	23	09	8.68	83.61	5.6	5.2	28	120	123
1990	07	23	05	27	04	9.33	84.80	5.5	5.1	25	82	86
1990	12	22	17	27	54	9.91	84.31	5.9	5.6	5	36	37
1990	12	22	17	28	45	9.85	84.31	5.5	5.1	5	31	31
1991	04	22	01	00	00	9.61	83.15	6.5	6.5	10	106	106
1991	04	22	02	00	00	9.61	83.15	7.0	7.3	10	106	106

(Note) M_b : Body Wave Magnitude H : Focal Depth (km)
 M_s : Surface Wave Magnitude D : Epicentral Distance (km)
 M_L : Local Magnitude R : Hypocentral Distance (km)

Table 8-3 Historical Earthquakes in the Vicinity of Pirris Project Site

No.	Fecha	Lat. N	Long. W.	Mag.	Fuente	Dist. (km)
01	02/09/1841	09 50.50	83 54.60	M =5.8	F	41
02	18/03/1851	10 08.00	84 11.70	M =5.5	F	50
03	30/12/1888	10 08.00	84 11.70	M =5.2	F	50
04	20/01/1905	09 51.00	84 40.80	Ms=6.7	S	64
05	13/04/1910	09 50.10	84 01.60	M =5.2	F	27
06	04/05/1910	09 50.50	83 54.60	M =5.5	F	40
07	29/08/1911	10 14.00	84 18.00	M =5.5	F	65
08	21/02/1912	09 52.00	84 00.00	M =5.0	F	38
09	06/06/1912	10 01.50	84 16.50	M =5.5	F	42
10	24/04/1916	10 08.40	84 37.80	Ms=7.3	S	73
11	04/03/1924	09 51.00	84 33.60	Ms=7.0	S	48
12	18/06/1939	10 00.00	84 06.00	Ms=6.5	F	46
13	21/12/1939	10 08.40	84 36.00	Ms=7.3	S	70
14	22/12/1939	09 48.00	84 31.80	Ms=6.7	S	45
15	27/10/1940	09 45.00	84 30.00	Ms=6.7	S	37
16	21/08/1951	09 48.05	83 52.90	M =5.0	F	34
17	09/09/1952	09 12.00	84 12.00	Ms=7.0	S	48
18	30/12/1952	10 01.50	83 54.50	M =5.5	F	49
19	01/09/1955	10 14.00	84 19.60	M =5.8	F	67
20	09/04/1966	09 12.00	84 14.40	Mb=5.3	S	48
21	05/08/1971	09 12.60	84 15.00	Mb=5.0	S	49
22	04/08/1973	09 27.60	84 51.60	Mb=5.1	S	83
23	25/11/1976	09 25.80	84 52.80	Mb=5.1	S	81
24	01/12/1976	09 27.00	84 55.90	Mb=5.3	S	82
25	17/08/1982	09 12.60	84 14.40	Mb=5.4	S	47
26	03/07/1983	09 30.60	83 40.02	Ms=6.2	F	55
27	25/09/1985	09 02.63	84 02.57	Mb=5.2		56
28	31/01/1988	09 47.24	83 47.68	Mb=5.4		40
29	02/03/1988	09 31.77	84 52.30	Mb=5.5		89
30	26/02/1989	09 38.97	84 13.26	Mb=5.4		25
31	25/03/1990	09 35.17	84 56.26	Mb=6.5		93
32	25/03/1990	09 32.53	84 56.66	Mb=5.7		95
33	30/06/1990	09 49.50	84 22.86	Mb=5.4		36
34	23/07/1990	09 20.24	84 47.61	Mb=5.5		86
35	22/12/1990	09 54.66	84 18.77	Mb=5.9		37

* Fuentes: F = Falla, S = Proceso de subduccion

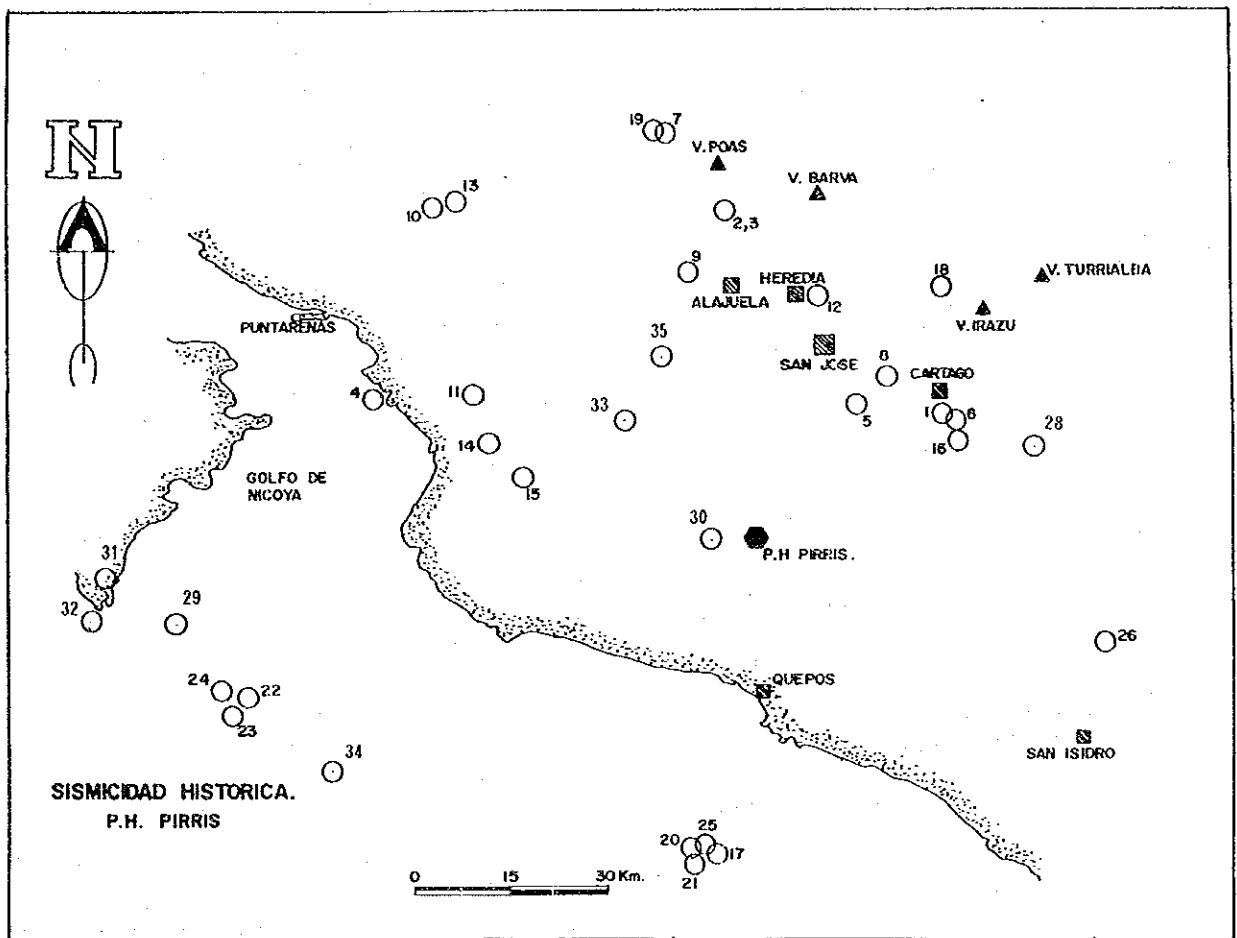


Fig. 8-3 Historical Earthquakes in the Vicinity of Pirris Project Site

8.2.2 Seismic Risk Analysis Based on Stochastic Technique

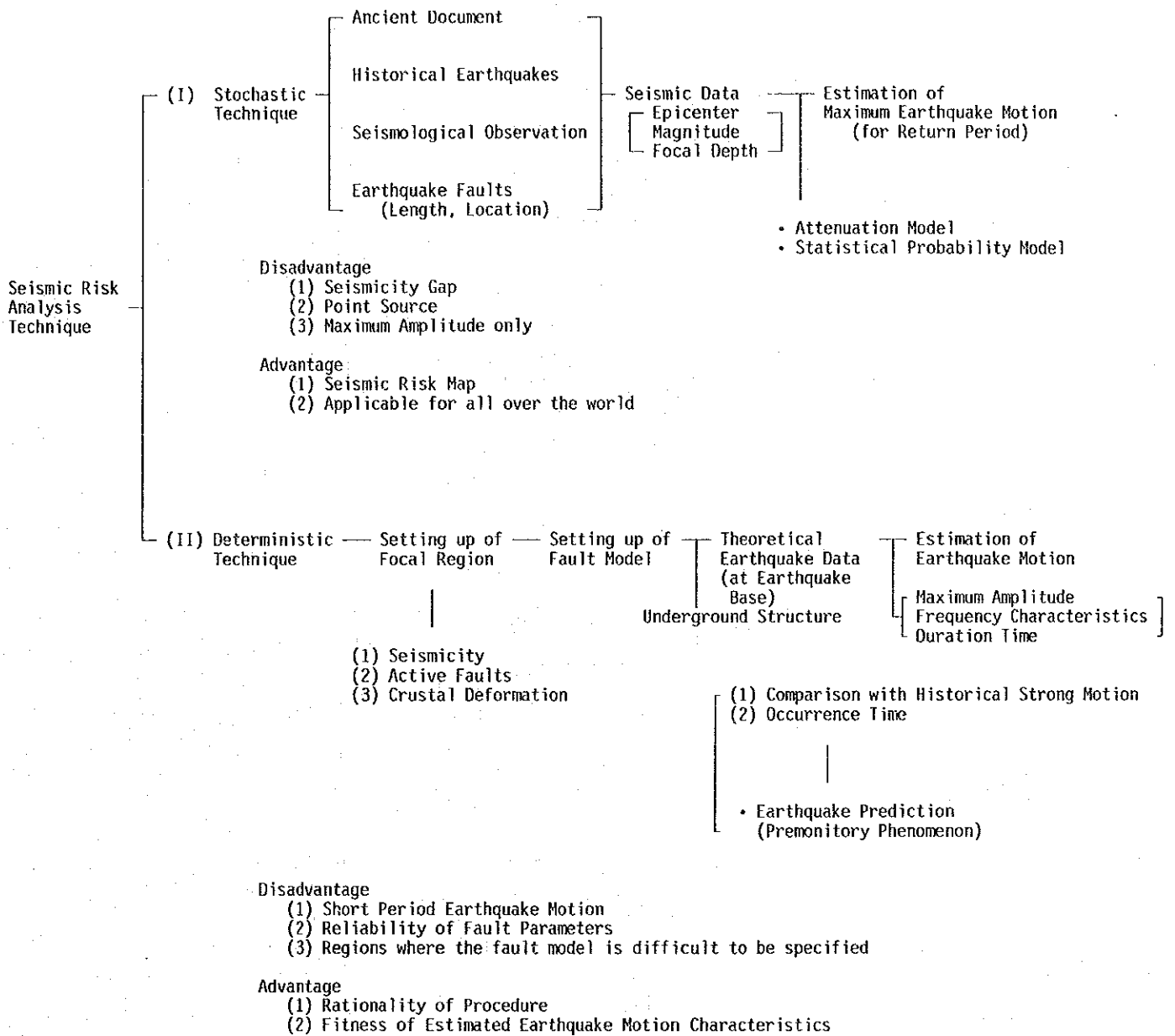
(1) Outline of Analysis

Evaluation techniques for seismic risk analyses, as shown in Fig. 8-4, may be broadly divided into stochastic technique and deterministic technique.

A stochastic technique is a method for estimating the maximum acceleration which may be expected in any return period based on data of historical earthquakes occurred using attenuation models and stochastic models. This technique has good reliability when enough earthquake data are available, and is presently the most generally used method. This technique can be also applied to the seismic risk evaluation based on the earthquake faults by estimating the magnitude from the length of the faults in case the location of the earthquake faults and the length are known.

On the other hand, a deterministic technique is a method for estimating the earthquake motion assumable for the site by numerical analysis setting up the fault models for earthquakes based on the seismic activity (aftershock area, periodicity), distribution of earthquake faults, crustal movements, and on consideration of the underground structure. It is possible with this method to obtain a rational result if the conditions necessary for analyses can be assumed properly. However in general, it is very difficult for estimation of fault parameters or underground structures at present level. Furthermore, the estimation of short-period components (roughly, shorter than 1 sec) cannot be adequately done at the present time. So it is not necessarily a generally-used method for practical purposes, although there are some cases of application for research purposes.

Taking into account the advantages and disadvantages of the analysis techniques described above, it was decided for the seismic risk analysis to be made by a stochastic technique because of plentiful data of historical earthquakes with regard to the Pirris project site.



**Fig. 8-4 Seismic Risk Analysis Techniques
(Stochastic Technique and Deterministic Technique)**

(2) Analysis Method

(i) Gumbel's Extreme Value Theory

Assuming that the stochastic variable x follows the stochastic function $G(X)$:

$$G(x) = Q(X \leq x)$$

The probability that x will be larger than any of $X_1, X_2 \dots X_n$ is defined as follows:

$$\begin{aligned} P_n(x) &= Q(X_1 \leq X, X_2 \leq X, \dots X_n \leq X) \\ &= G_n(X) \end{aligned}$$

At this time, the return period $P(x)$ and the conversion variable z will be expressed as follows:

$$\begin{aligned} P(x) &= 1/\{1 - P_n(x)\} \\ Z &= -\ln \{1 - 1_n P_n(x)\} \end{aligned}$$

Gumbel's extreme value theory (1958) can be applied even when the original distribution of the stochastic variable is unknown. But in case of applying the extreme value theory to earthquake phenomena, the frequency of earthquake occurrence, and the return period can be predicted and evaluated if the following hypothetical conditions are satisfied:

Hypothesis (1) The pattern of earthquake occurrence in the past will continue without failure in the future.

Hypothesis (2) The maximum earthquake phenomenon observed in the given time interval is an independent phenomena.

Hypothesis (3) The future trend of occurrence of maximum earthquake in the given time interval is the same as in the past.

In Gumbel's extreme value theory, three kinds of extreme asymptotic distributions are proposed according to the behavior characteristics of maximum value of stochastic variables.

1st Asymptotic Distribution

$$P_n(x) = \exp \{-\exp(-\alpha_n)(x-V)\}$$

2nd Asymptotic Distribution

$$P_n(x) = \exp \{[-(V-\varepsilon)/(x-\varepsilon)]k\}$$

3rd Asymptotic Distribution

$$P_n(x) = \exp \{[-(W-x)/(W-V)]k\}$$

There is no upper limit or lower limit for the stochastic variable in the 1st asymptotic distribution. With the 2nd asymptotic distribution, there is a lower limit for stochastic variables, and with the 3rd asymptotic distribution, an upper limit.

Incidentally, the stochastic function of maximum acceleration assumed for the site considered here is unknown. However, since it may be considered that there is an upper limit to the maximum amplitude of earthquake motion at any site, it can be judged to be reasonable to apply the 3rd asymptotic distribution. In the 3rd asymptotic distribution equation, w is the upper limit of maximum amplitude, k is a shape factor, V is the maximum value of characteristic, and x is a random stochastic variable. With A_{\max} as the maximum acceleration of earthquake motion at a certain site in a unit period of time, x is expressed by the following equation:

$$x = \log A_{\max}$$

And, the plotted location of maximum acceleration in a unit period of time is obtained by the following equation:

$$P(m) = (N - m + 1) / (N + 1)$$

Where, N indicates the number of unit periods for the analysis, and m the order of rank from the maximum value.

(ii) Earthquake Data

In the seismic risk analysis here, the earthquake data from the earthquake data file of NOAA (National Oceanic and Atmospheric Administration of the United States Geophysical Data Center) were used.

The earthquakes occurred within a radius of 1,000 km from the Pirris project site during the period from 1900 to 1991 and were 5,191 in number.

A radius of 1,000 km was set here as the object of evaluation, and when the damping characteristics of maximum acceleration of earthquake motion is considered, it is a range which is adequate for evaluation. The numbers of earthquakes which occurred in each year during the period from 1900 to 1991 are given in Table 8-4. The distribution of earthquake magnitudes and epicentral distance used in the stochastic analyses are as shown in Table 8-5.

Table 8-4 Annual Number of Earthquakes during 1900-1991
 $D \leq 1,000$ km ($D =$ Epicentral Distance)

YEAR	N	SUM of N	YEAR	N	SUM of N
1902	2	2	1952	14	194
1904	4	6	1953	5	199
1906	2	8	1954	11	210
1907	1	9	1955	6	216
1909	1	10	1956	12	228
1910	1	11	1957	9	237
1912	1	12	1958	7	244
1913	1	13	1959	9	253
1914	2	15	1960	10	263
1915	2	17	1961	12	275
1916	5	22	1962	11	286
1919	4	26	1963	101	387
1920	2	28	1964	171	558
1921	4	32	1965	166	724
1924	5	37	1966	147	871
1925	5	42	1967	139	1010
1926	6	48	1968	80	1090
1927	2	50	1969	96	1186
1929	2	52	1970	113	1299
1930	1	53	1971	75	1374
1931	10	63	1972	87	1461
1932	5	68	1973	132	1593
1933	11	79	1974	188	1781
1934	13	92	1975	116	1897
1935	4	96	1976	237	2134
1936	2	98	1977	106	2240
1937	6	104	1978	118	2358
1939	10	114	1979	209	2567
1940	4	118	1980	141	2708
1941	11	129	1981	112	2820
1942	7	136	1982	168	2988
1943	6	142	1983	135	3123
1944	3	145	1984	124	3247
1945	4	149	1985	132	3379
1946	3	152	1986	125	3504
1947	2	154	1987	189	3693
1948	2	156	1988	220	3913
1949	2	158	1989	311	4224
1950	8	166	1990	924	5148
1951	14	180	1991	43	5191

Table 8-5 Distribution of Magnitude and Epicentral Distance of Earthquakes during 1900-1991

M \ D	0<=D<50	<100	<200	<300	<400	<500	<600	<700	<800	<1000	1000<=	TOTAL
0<M<3.0	0	0	0	0	0	0	0	0	0	0	0	0
<3.5	377	319	133	17	1	1	0	0	0	0	0	848
<4.0	153	131	120	39	8	5	17	13	14	83	0	583
<4.5	56	56	77	87	83	63	103	103	171	357	0	1156
<5.0	37	45	94	103	151	102	145	160	222	556	0	1615
<5.5	13	14	33	41	59	45	46	59	72	203	0	585
<6.0	6	0	7	13	15	11	11	7	11	48	2	131
<6.5	2	0	5	13	17	14	13	11	12	40	0	127
<7.0	4	6	9	7	16	12	9	7	6	32	0	108
<7.5	0	0	9	2	4	3	0	6	3	3	0	30
<8.0	0	0	2	0	0	0	0	0	0	4	0	6
8.0<=	0	0	0	0	0	0	0	0	0	2	0	2
UNKNOWN	0	0	0	0	0	0	0	0	0	0	0	0
TOTAL	648	571	489	322	354	256	344	366	511	1328	2	5191

D : Epicentral Distance (Km)
M : Magnitude

(iii) Attenuation Model

The equations for attenuation with distance applied in prediction of maximum acceleration were the four below out of those proposed up to the present.

The "A" in each equation depicts maximum acceleration (gal), the "M" magnitude of earthquake, and the "R" hypocentral distance (km).

$$\text{Log A} = 3.090 + 0.347M - 2 \text{ Log (R+25)} \dots \dots \dots (1)$$

Proposed by C. Oliveira

$$\text{Log A} = 2.647 + 0.278 M - 1.301 \text{ Log (R+25)} \dots \dots \dots (2)$$

Proposed by P. K. McGuire

$$\text{Log A} = 2.041 + 0.347 M - 1.6 \text{ Log R} \dots \dots \dots (3)$$

Proposed by L. Esteva and E. Rosenblueth

$$\text{Log A} = 2.308 + 0.411 M - 1.637 \text{ Log (R+30)} \dots \dots \dots (4)$$

Proposed by T. Katayama

(3) Analysis Results

The data of 5,191 earthquakes during the 92-year period from 1900 to 1991 were used for prediction of maximum acceleration by stochastic analysis. Here, the isochronal interval of the probability model based on the "Gumbel's extreme value theory" was taken as 1 year. Although the probability relationship of maximum acceleration expected at the Pirris project site is unknown, since it is logical to consider that there is an upper limit to the value of maximum acceleration at the site, as previously stated, a third asymptotic distribution was assumed.

Regarding the maximum accelerations of the Pirris project site evaluated using the equations of Oliveira, McGuire, Esteva-Rosenblueth, and Katayama, the largest maximum acceleration values evaluated for each of the 92 years from 1900 to 1991 are given in Table 8-6.

The analytical results of maximum accelerations for the return periods are shown in Fig. 8-5 (Oliveira's equation), Fig. 8-6 (McGuire's equation), Fig. 8-7 (Esteva-Rosenblueth's equation), and Fig. 8-8 (Katayama's equation).

Table 8-6 (1) Annual Maximum Accelerations during 1900-1991

YEAR	ATTENUATION MODEL			
	OLIVEIRA	MCGUIRE	ESTEVA & ROSENBLUETH	KATAYAMA
1900	0.0	0.0	0.0	0.0
1901	0.0	0.0	0.0	0.0
1902	0.71	9.33	1.01	4.29
1903	0.0	0.0	0.0	0.0
1904	14.30	66.01	13.21	48.85
1905	0.0	0.0	0.0	0.0
1906	0.76	10.28	1.14	5.12
1907	2.23	18.14	2.41	8.89
1908	0.0	0.0	0.0	0.0
1909	32.80	103.36	29.32	74.07
1910	0.64	8.27	0.87	3.43
1911	0.0	0.0	0.0	0.0
1912	0.28	4.56	0.41	1.53
1913	1.25	11.61	1.37	4.69
1914	0.69	8.44	0.90	3.43
1915	0.87	10.37	1.16	4.73
1916	20.08	76.31	17.70	52.55
1917	0.0	0.0	0.0	0.0
1918	0.0	0.0	0.0	0.0
1919	2.07	16.40	2.15	7.34
1920	1.56	13.13	1.63	5.31
1921	1.37	13.30	1.61	6.10
1922	0.0	0.0	0.0	0.0
1923	0.0	0.0	0.0	0.0
1924	91.11	199.47	101.68	159.03
1925	2.10	16.82	2.21	7.75
1926	1.96	16.40	2.12	7.69
1927	0.95	10.22	1.15	4.27
1928	0.0	0.0	0.0	0.0
1929	1.86	14.71	1.90	6.11
1930	0.55	6.79	0.69	2.39
1931	2.18	16.33	2.18	6.95
1932	2.12	16.93	2.23	7.81
1933	3.05	20.27	2.92	9.08
1934	5.51	33.92	5.46	20.25
1935	0.66	7.63	0.80	2.77
1936	4.81	26.49	4.35	12.11
1937	13.80	55.82	12.15	32.64
1938	0.0	0.0	0.0	0.0
1939	33.77	102.59	30.75	70.53
1940	57.76	140.13	62.50	95.94
1941	11.99	52.95	10.68	32.31
1942	0.88	9.32	1.01	4.29
1943	0.90	9.99	1.12	4.19
1944	1.25	11.34	1.34	4.42
1945	5.80	33.25	5.48	18.44
1946	0.27	4.39	0.39	1.42
1947	1.69	15.15	1.90	7.11
1948	16.45	65.52	14.52	42.29
1949	5.75	31.87	5.32	16.66
1950	10.36	51.13	9.58	33.58
1951	1.41	12.22	1.46	5.33
1952	41.04	117.60	37.99	84.20
1953	0.39	5.86	0.56	2.20
1954	1.27	12.05	1.43	5.06

Table 8-6 (2) Annual Maximum Accelerations during 1900-1991

YEAR	ATTENUATION MODEL			
	OLIVEIRA	MCGUIRE	ESTEVA & ROSENBLUETH	KATAYAMA
1955	0.81	8.70	0.95	3.26
1956	29.62	89.03	27.90	54.61
1957	5.75	31.87	5.32	16.66
1958	5.87	32.87	5.48	17.73
1959	1.92	15.45	2.00	6.73
1960	1.98	16.10	2.09	7.26
1961	9.40	40.25	8.28	19.69
1962	4.53	27.75	4.33	14.39
1963	5.09	22.58	4.63	7.54
1964	6.41	25.60	6.18	8.43
1965	6.02	24.01	5.94	7.81
1966	19.84	63.97	18.90	33.10
1967	1.80	13.60	1.76	5.14
1968	3.65	19.78	3.22	7.27
1969	11.77	38.95	12.92	14.33
1970	6.41	25.91	6.09	9.19
1971	19.30	60.60	20.30	29.31
1972	4.42	23.52	3.92	9.60
1973	14.33	45.91	15.49	18.44
1974	18.84	62.61	17.56	32.88
1975	4.43	20.61	3.97	6.77
1976	12.79	43.65	12.72	18.09
1977	8.12	32.49	7.44	12.76
1978	20.65	57.51	27.78	23.41
1979	8.80	39.56	7.76	19.98
1980	7.75	30.04	7.41	10.79
1981	5.30	23.17	4.84	8.05
1982	16.99	55.78	16.46	26.59
1983	20.70	67.37	19.33	36.54
1984	12.33	42.13	12.41	17.02
1985	11.85	43.09	11.07	18.87
1986	4.47	22.00	3.95	7.97
1987	12.08	40.58	12.66	15.65
1988	22.48	67.34	34.51	33.49
1989	38.97	96.30	83.43	50.65
1990	45.41	98.31	165.51	57.43
1991	45.52	105.65	69.22	55.42

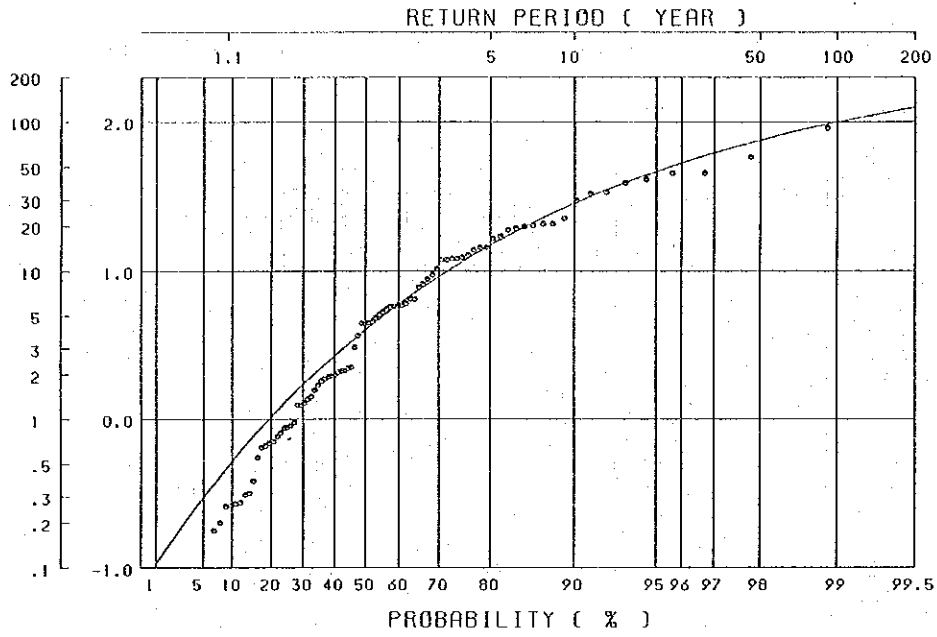
【Attenuation Model】

[1] : $\text{Log}A = 3.09 + 0.347M - 21.0 \log (R+25)$ (by Oliveira)

[2] : $\text{Log}A = 2.674 + 0.278M - 1.301 \log (R+25)$ (by McGuire)

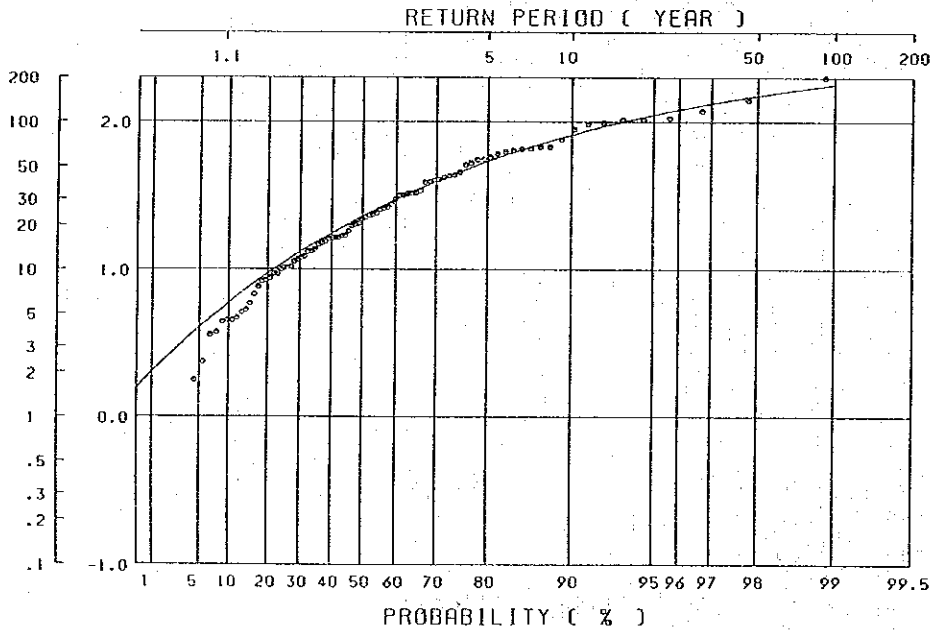
[3] : $\text{Log}A = 2.041 + 0.347M - 1.6 \log (R)$ (by Esteva & Rosenblueth)

[4] : $\text{Log}A = 2.308 + 0.411M - 1.637 \log (R+30)$ (by Katayama)



1: $\text{LOG } A = 3.09 + 0.347M - 2\text{LOG}(R+25)$ (C. OLIVEIRA)

Fig. 8-5 Return Period for Maximum Acceleration calculated by Eq. (1)



2: $\text{LOG } A = 2.674 + 0.278M - 1.301\text{LOG}(R+25)$

(R.K. MCGUIRE)

Fig. 8-6 Return Period for Maximum Acceleration calculated by Eq. (2)